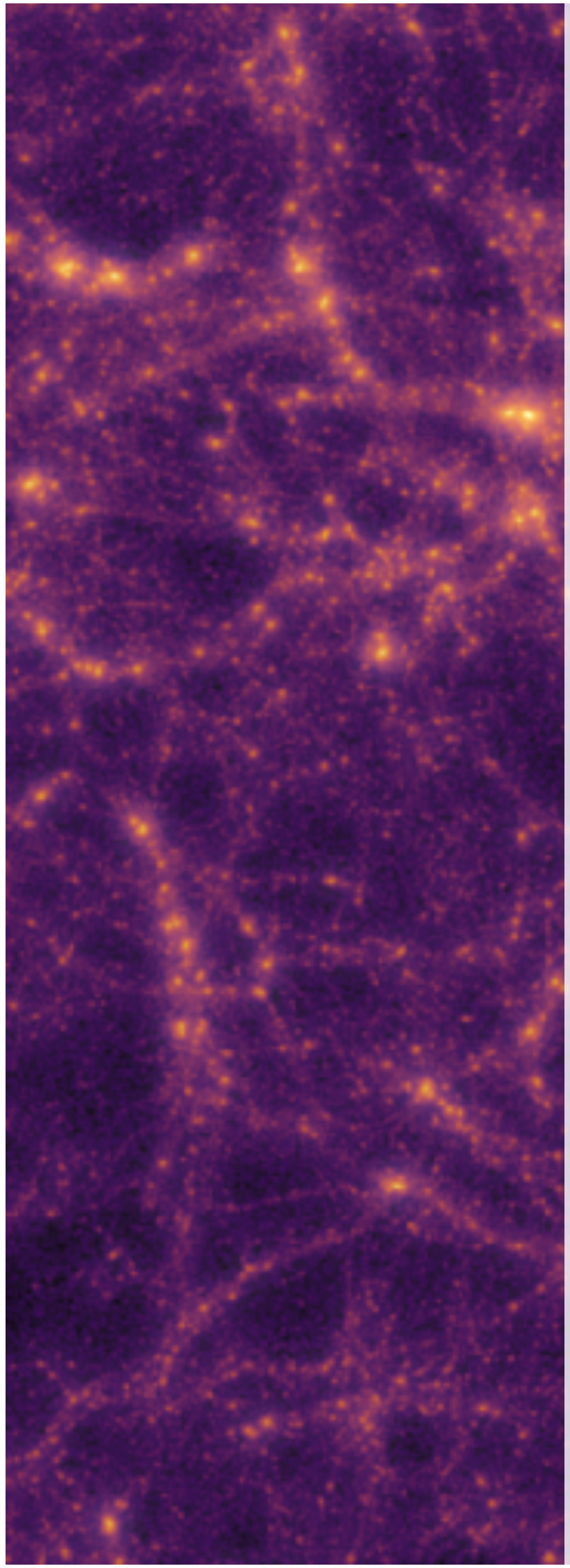

Evolution mapping: a tool to describe non-linear density fluctuations

Ariel G. Sánchez
MPE/LMU

C. Correa, A. Eggemeier, M. Esposito, L. Finkbeiner, A. Fiorilli, A. Perez Fernandez, A. Pezzotta, A. Ruiz, A. Semenaite

New Strategies for Extracting Cosmology from Galaxy Surveys II - July 2024

New LSS analysis methods

State-of-the-art models only access large-scale information.

New surveys exacerbate this problem.

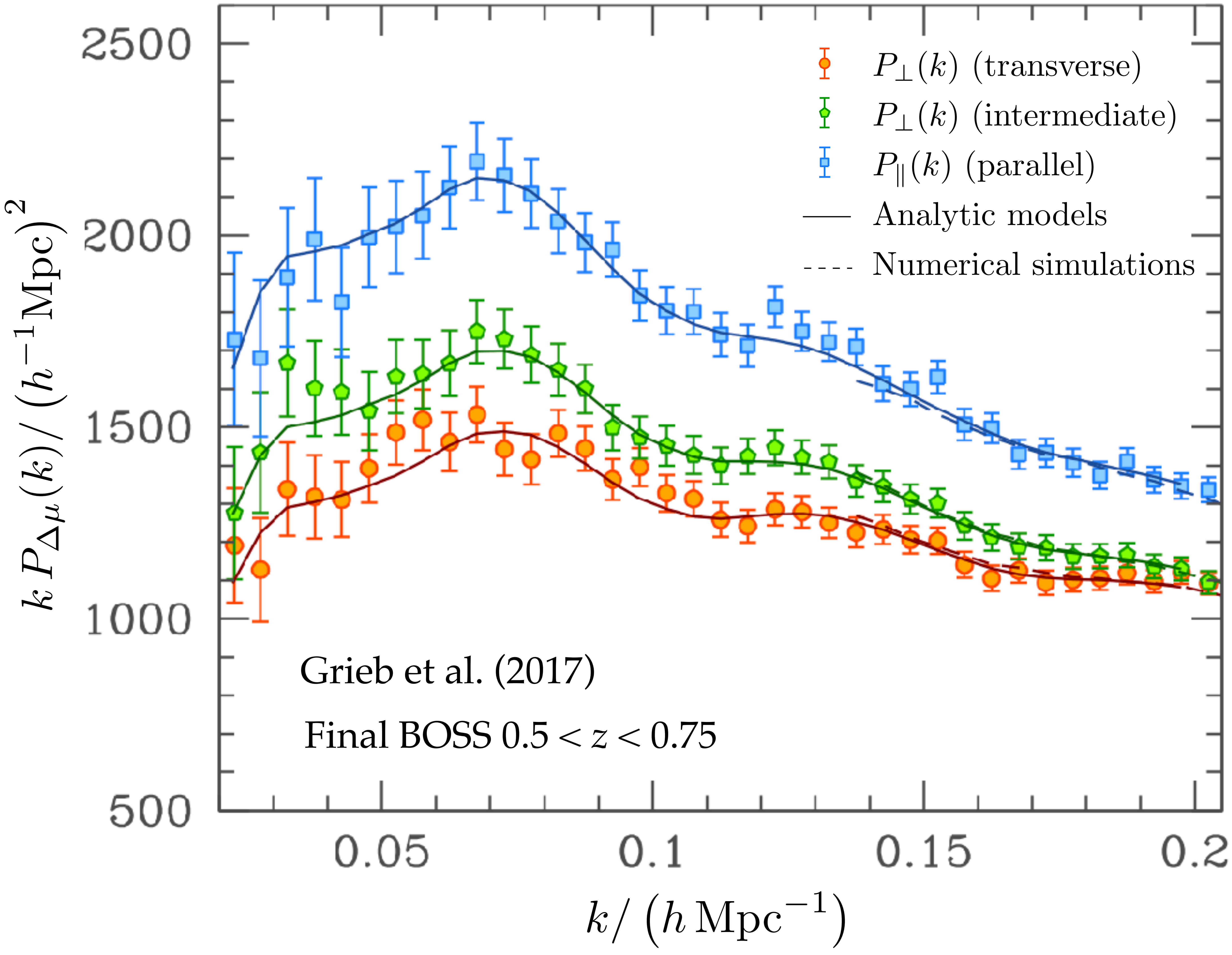

Model predictions based on **simulations**:

Emulators trained on simulations.

Simulation-based inference.

Field-level inference.

Evolution mapping: linear $P(k)$

We can classify cosmological parameters according to their impact on $P(k)$

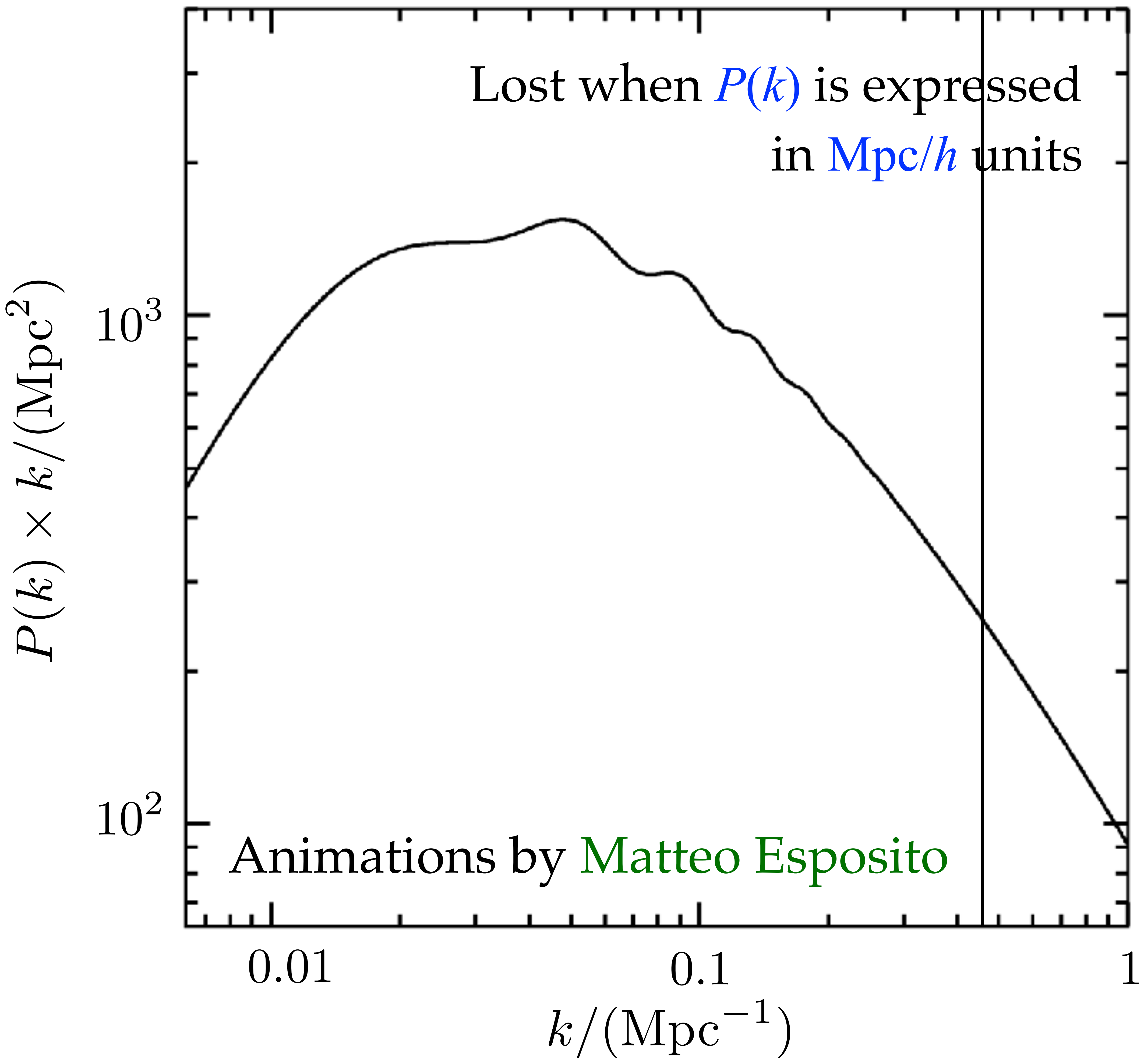

shape — evolution

$$\mathbf{\Theta} = (\omega_\mathrm{c}, \omega_\mathrm{b}, n_\mathrm{s}, A_\mathrm{s}, \omega_K, \omega_\mathrm{DE}, w_0, w_a, \ldots, z)$$

$$\mathbf{\Theta} = (\omega_\mathrm{c}, \omega_\mathrm{b}, n_\mathrm{s}, \sigma_{12})$$

$$h^2 = \sum_i \omega_i, \qquad \Omega_i = \omega_i / h^2,$$

$$\sigma_{8/h} = \sigma(R = 8/h\,\mathrm{Mpc})$$

$$\sigma_{12} = \sigma(R = 12\,\mathrm{Mpc})$$

$$P_\mathrm{L}(k|z, \mathbf{\Theta}_\mathrm{s}, \mathbf{\Theta}_\mathrm{e}) = P_\mathrm{L}\left(k|\mathbf{\Theta}_\mathrm{s}, \sigma_{12}\left(z, \mathbf{\Theta}_\mathrm{s}, \mathbf{\Theta}_\mathrm{e}\right)\right)$$

Alternative normalizations

The scale $R = 12\,\mathrm{Mpc}$ is arbitrary.

Alternative normalizations include:

- The value $\sigma(R)$ at any scale defined in Mpc.
- The value of $\Delta^2(k_\mathrm{p})$ at any scale k_p defined in Mpc^{-1}.
- The scale R_nl at which $\sigma(R_\mathrm{nl}) = 1$.
- The scale k_nl at which $\Delta^2(k_\mathrm{nl}) = 1$.

Evolution mapping: linear theory

We can map the z evolution of models with identical Θ_s using the value of σ_{12}

The Aletheia cosmologies

Model	Definition
Model 0	Reference ΛCDM as in Table 1.
Model 1	ΛCDM, $\omega_{DE} = 0.1594$ ($h = 0.55$).
Model 2	ΛCDM, $\omega_{DE} = 0.4811$ ($h = 0.79$).
Model 3	wCDM, $w_{DE} = -0.85$.
Model 3	wCDM, $w_{DE} = -1.15$.
Model 5	Dynamic dark energy, $w_a = -0.2$.
Model 6	Dynamic dark energy, $w_a = 0.2$.
Model 7	Non-flat ΛCDM, $\Omega_K = -0.05$.
Model 8	EDE model, $w_0 = -1.15$, $\Omega_{DE,e} = 10^{-5}$

Aletheia: greek godess of truth.
It means "*to reveal*".

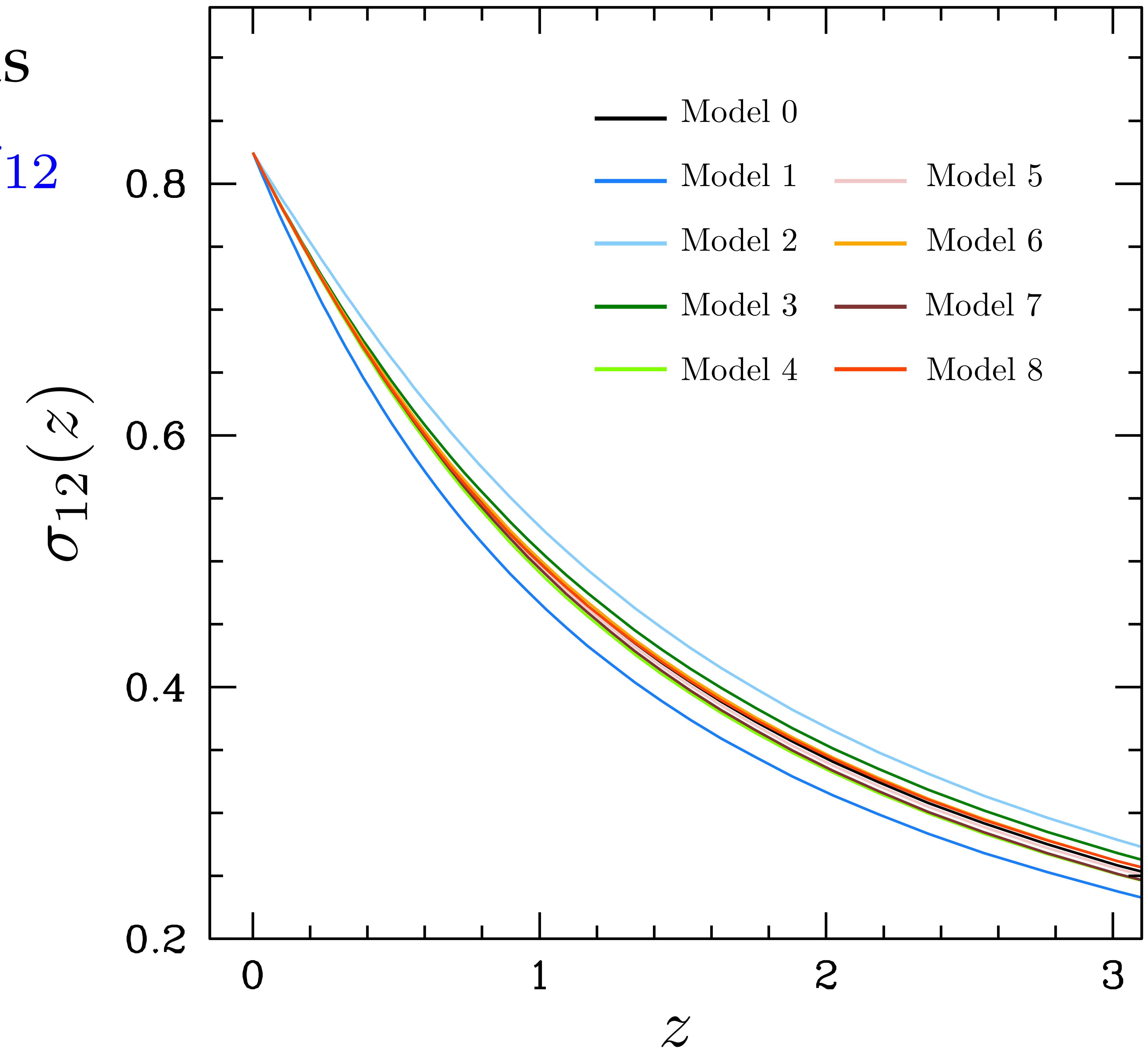

Evolution mapping: linear theory

We can map the z evolution of models with identical $\mathbf{\Theta}_\mathrm{s}$ using the value of σ_{12}

The Aletheia cosmologies

Model	Definition
Model 0	Reference ΛCDM as in Table 1.
Model 1	ΛCDM, $\omega_{\mathrm{DE}} = 0.1594$ ($h = 0.55$).
Model 2	ΛCDM, $\omega_{\mathrm{DE}} = 0.4811$ ($h = 0.79$).
Model 3	wCDM, $w_{\mathrm{DE}} = -0.85$.
Model 3	wCDM, $w_{\mathrm{DE}} = -1.15$.
Model 5	Dynamic dark energy, $w_a = -0.2$.
Model 6	Dynamic dark energy, $w_a = 0.2$.
Model 7	Non-flat ΛCDM, $\Omega_K = -0.05$.
Model 8	EDE model, $w_0 = -1.15$, $\Omega_{\mathrm{DE},e} = 10^{-5}$

Aletheia: greek godess of truth.
It means "*to reveal*".

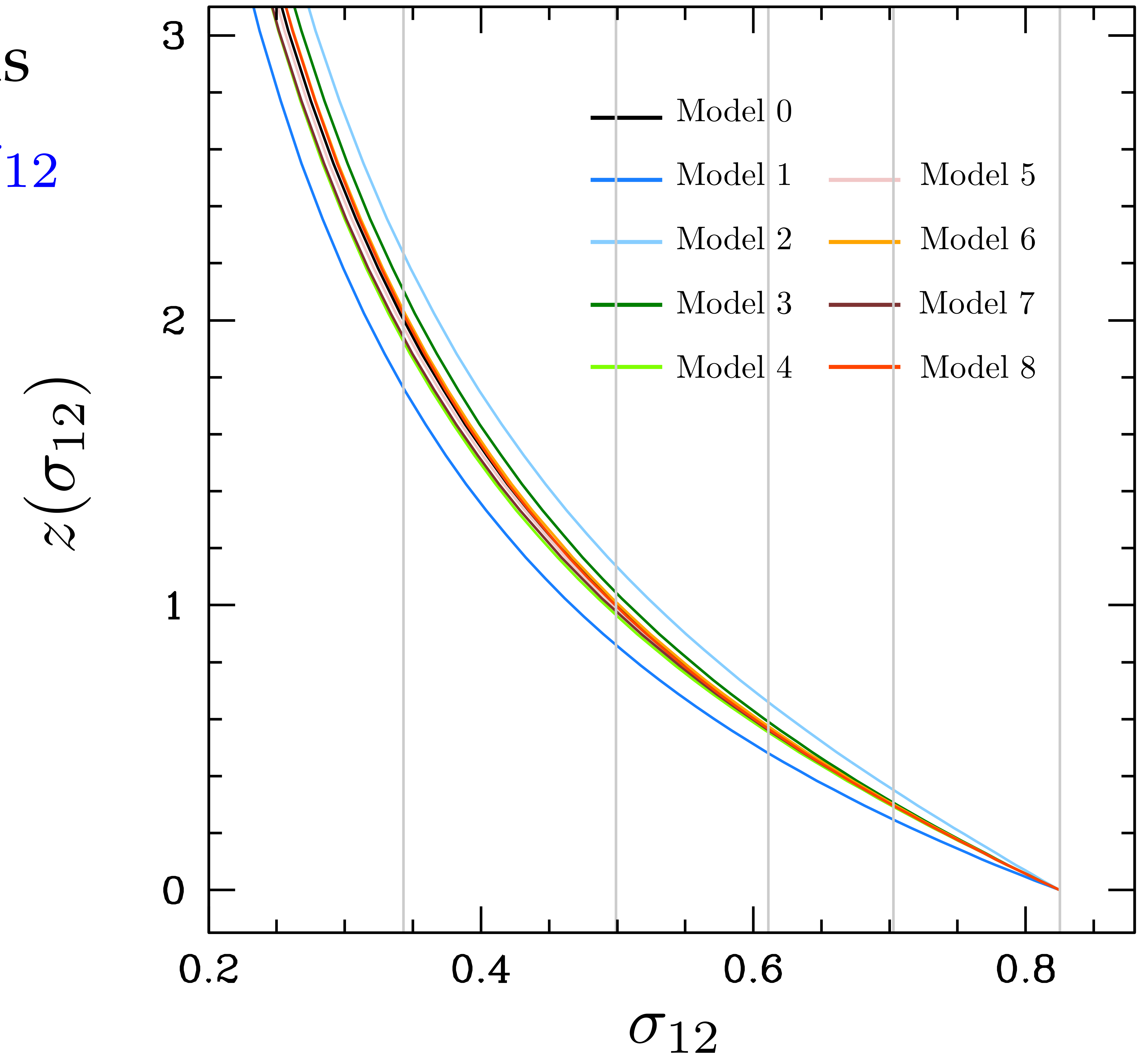

Evolution mapping: linear theory

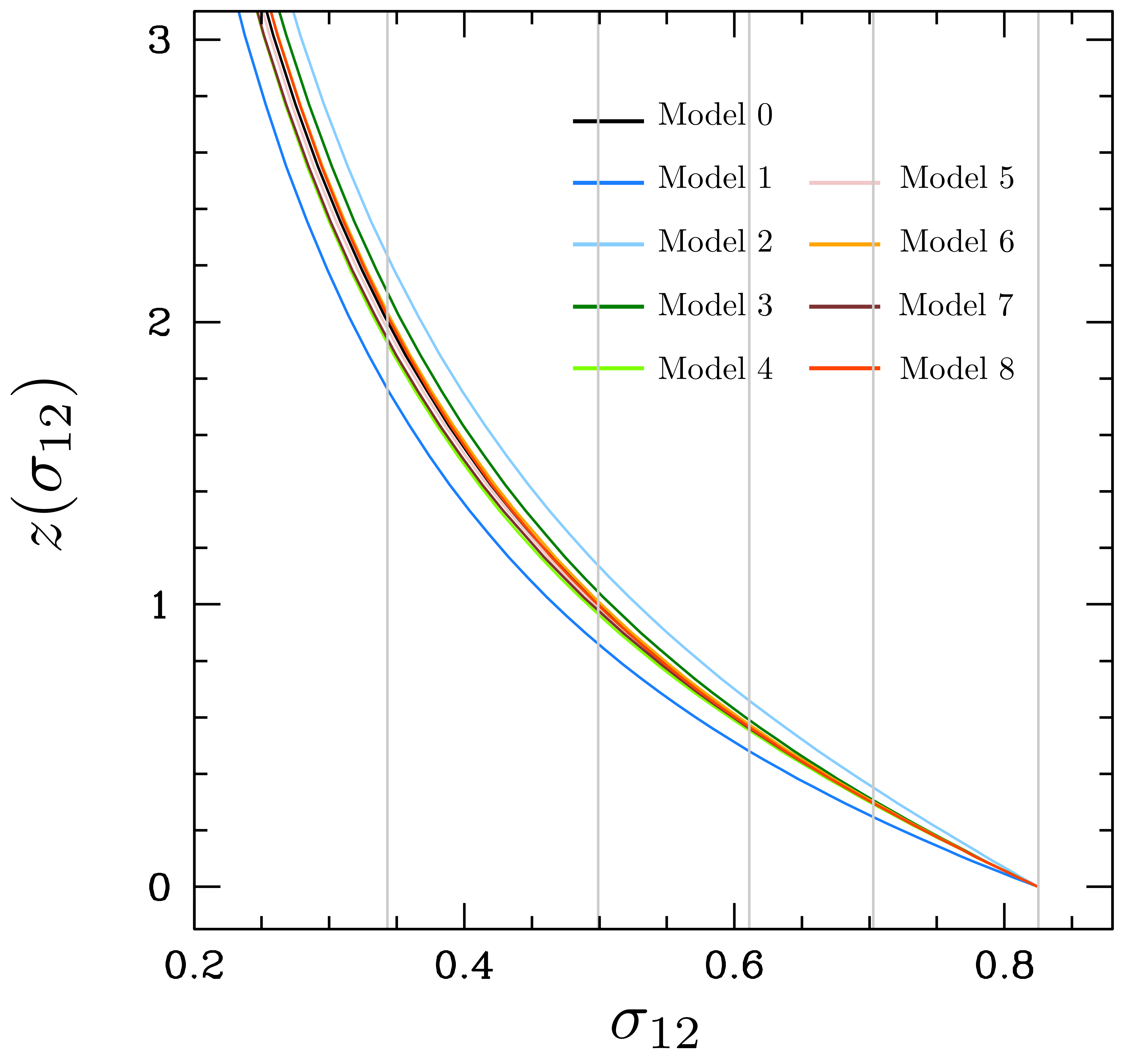

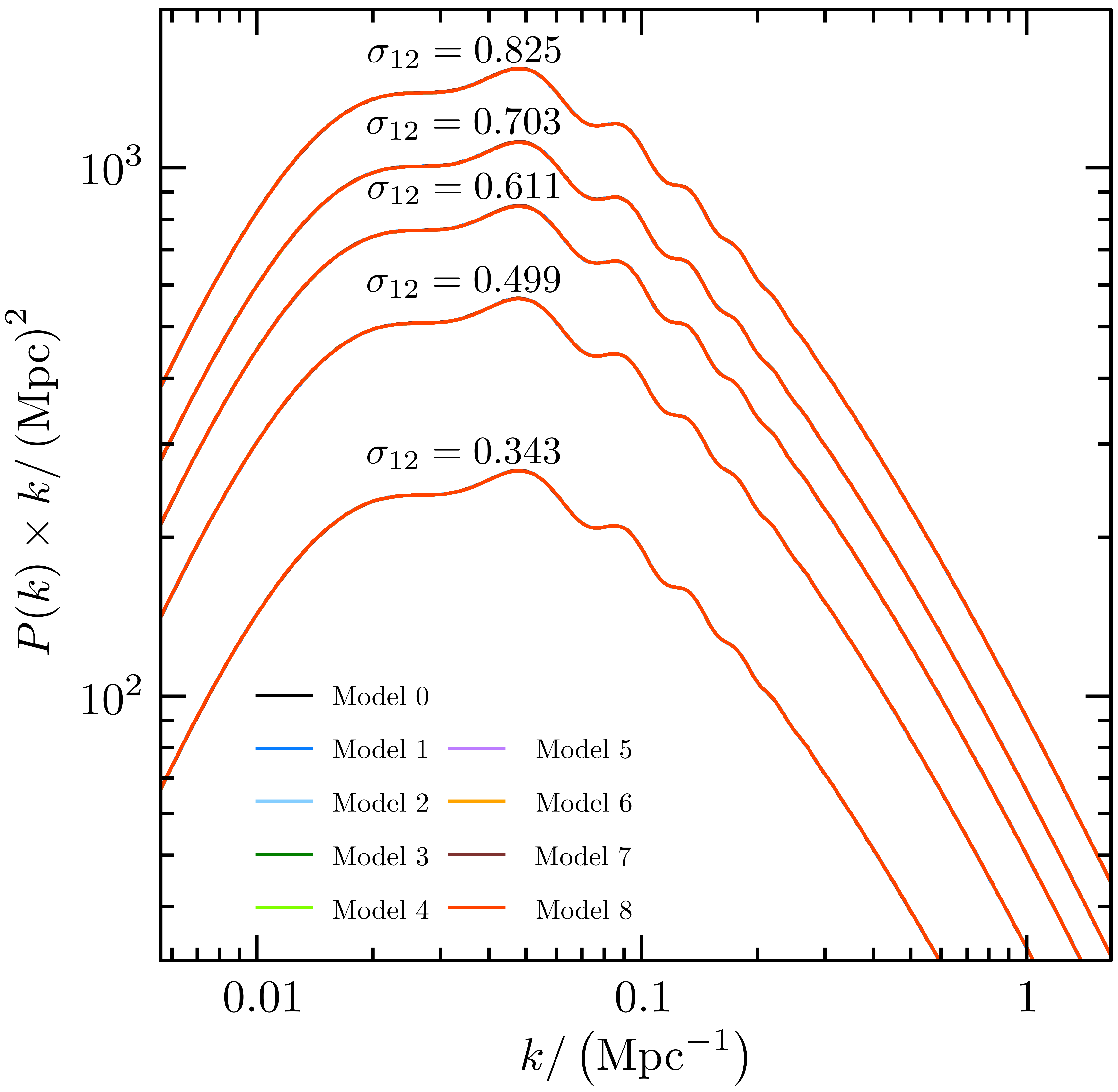

Evolution mapping: non-linear $P(k)$

- Evolution mapping gives a good description of the non-linear $P(k)$

$$P(k|z, \mathbf{\Theta}_{\rm s}, \mathbf{\Theta}_{\rm e}) \simeq P\left(k|\mathbf{\Theta}_{\rm s}, \sigma_{12}\left(z, \mathbf{\Theta}_{\rm s}, \mathbf{\Theta}_{\rm e}\right)\right)$$

- Differences can be seen in the deeply non-linear regime.
- Deviations are larger at high k and increase with σ_{12}.
- The models with the largest deviations change with σ_{12}.

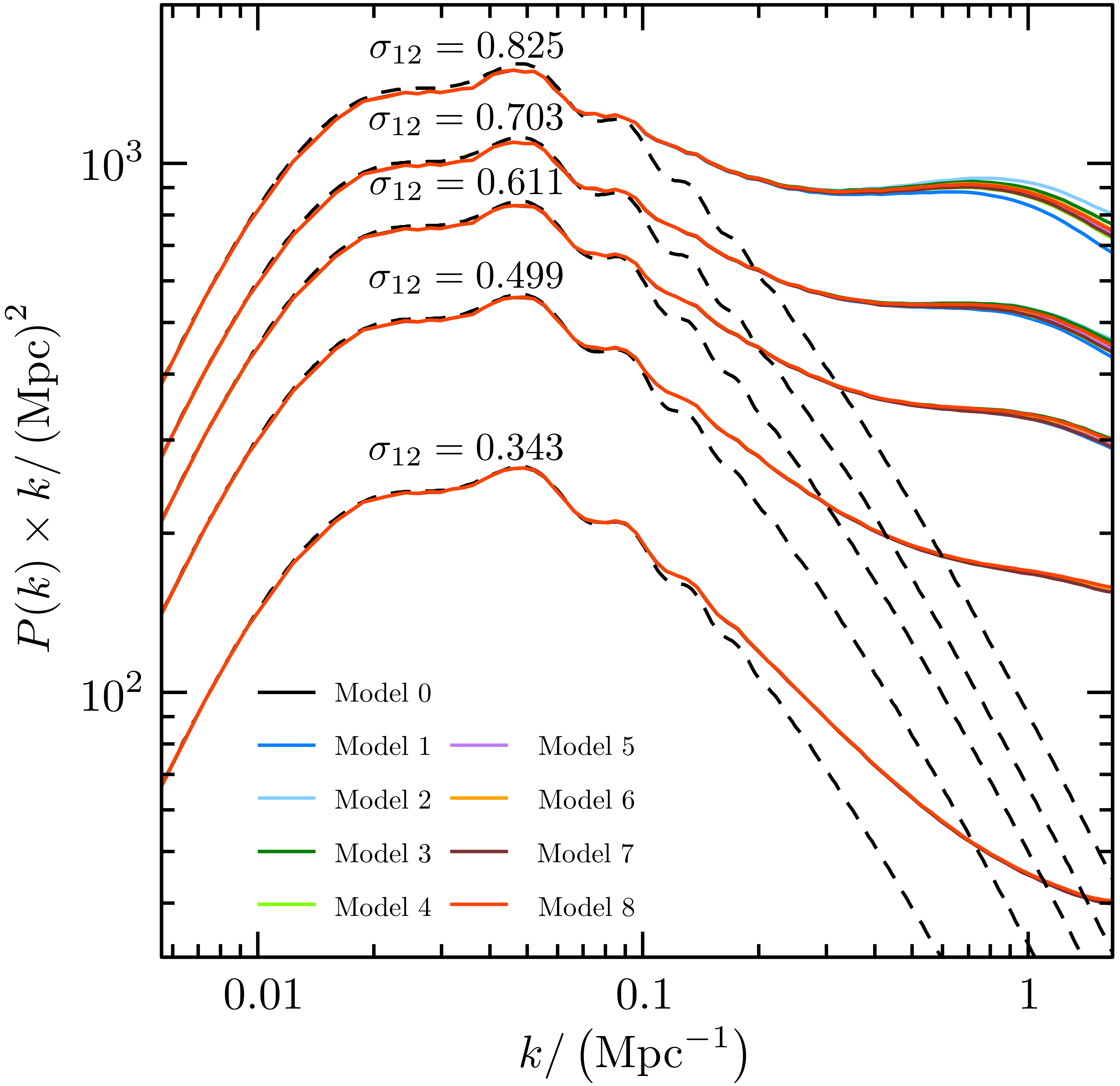

Evolution mapping: non-linear $P(k)$

- Evolution mapping gives a good description of the non-linear $P(k)$

$$P(k|z, \mathbf{\Theta}_\mathrm{s}, \mathbf{\Theta}_\mathrm{e}) \simeq P\left(k|\mathbf{\Theta}_\mathrm{s}, \sigma_{12}\left(z, \mathbf{\Theta}_\mathrm{s}, \mathbf{\Theta}_\mathrm{e}\right)\right)$$

- Differences can be seen in the deeply non-linear regime.
- Deviations are larger at high k and increase with σ_{12}.
- The models with the largest deviations change with σ_{12}.

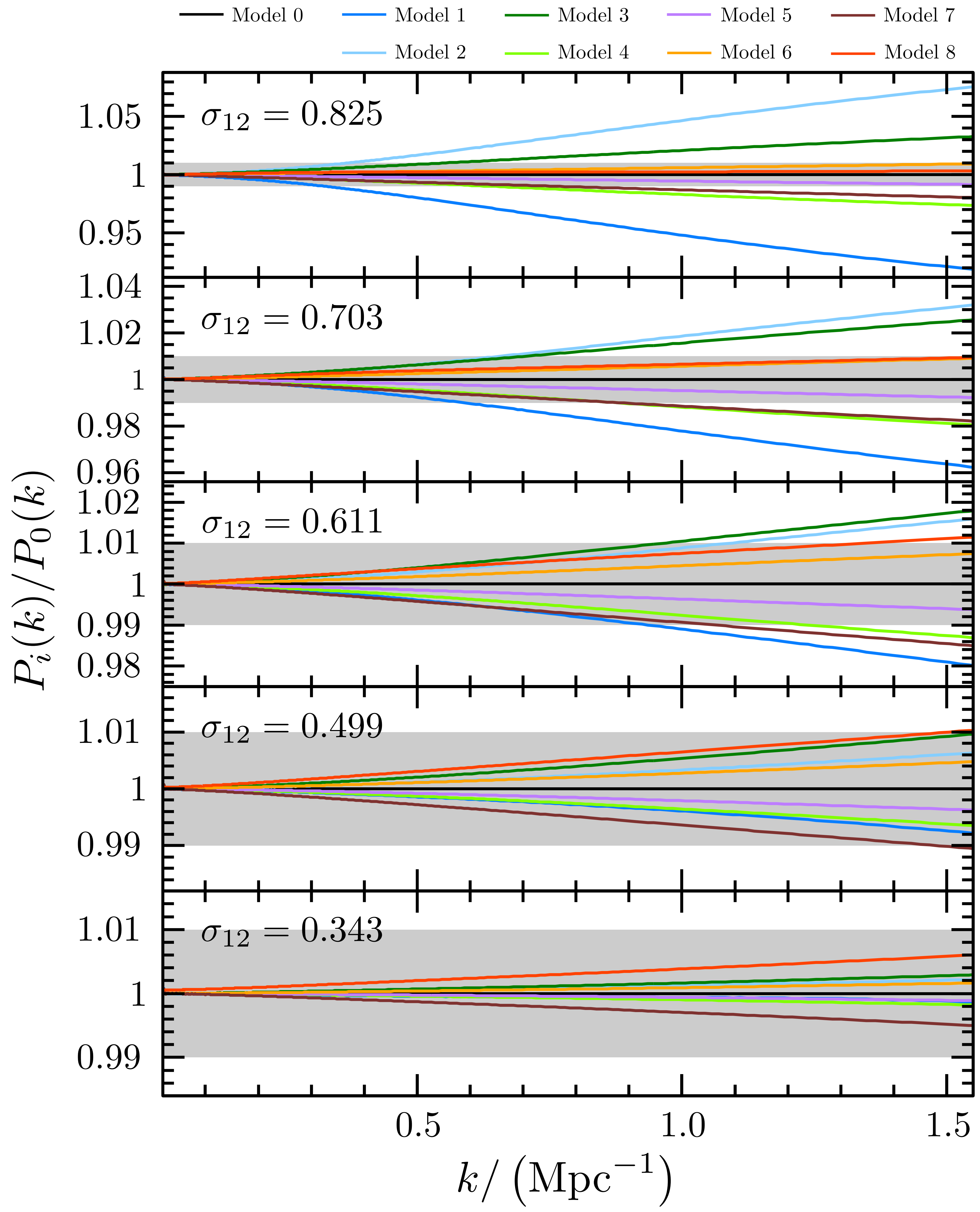

Deviations from the σ_{12} degeneracy

- The differences could be described as a functional of $g(a) = D(a)/a$

$$\delta P\left[\delta g(\sigma_{12})\right] = \int \frac{\delta P}{\delta g} \delta g(\sigma'_{12})\, \mathrm{d}\sigma'_{12}$$

- A simpler recipe:

$$P\left(k|g,g'\right) = P\left(k|g_0,g'_0\right) + \frac{\partial P}{\partial g}\left(k|g_0,g'_0\right)\left(g-g_0\right) + \frac{\partial P}{\partial g'}\left(k|g_0,g'_0\right)\left(g'-g'_0\right)$$

$$g' = \frac{\partial g}{\partial \ln \sigma_{12}}$$

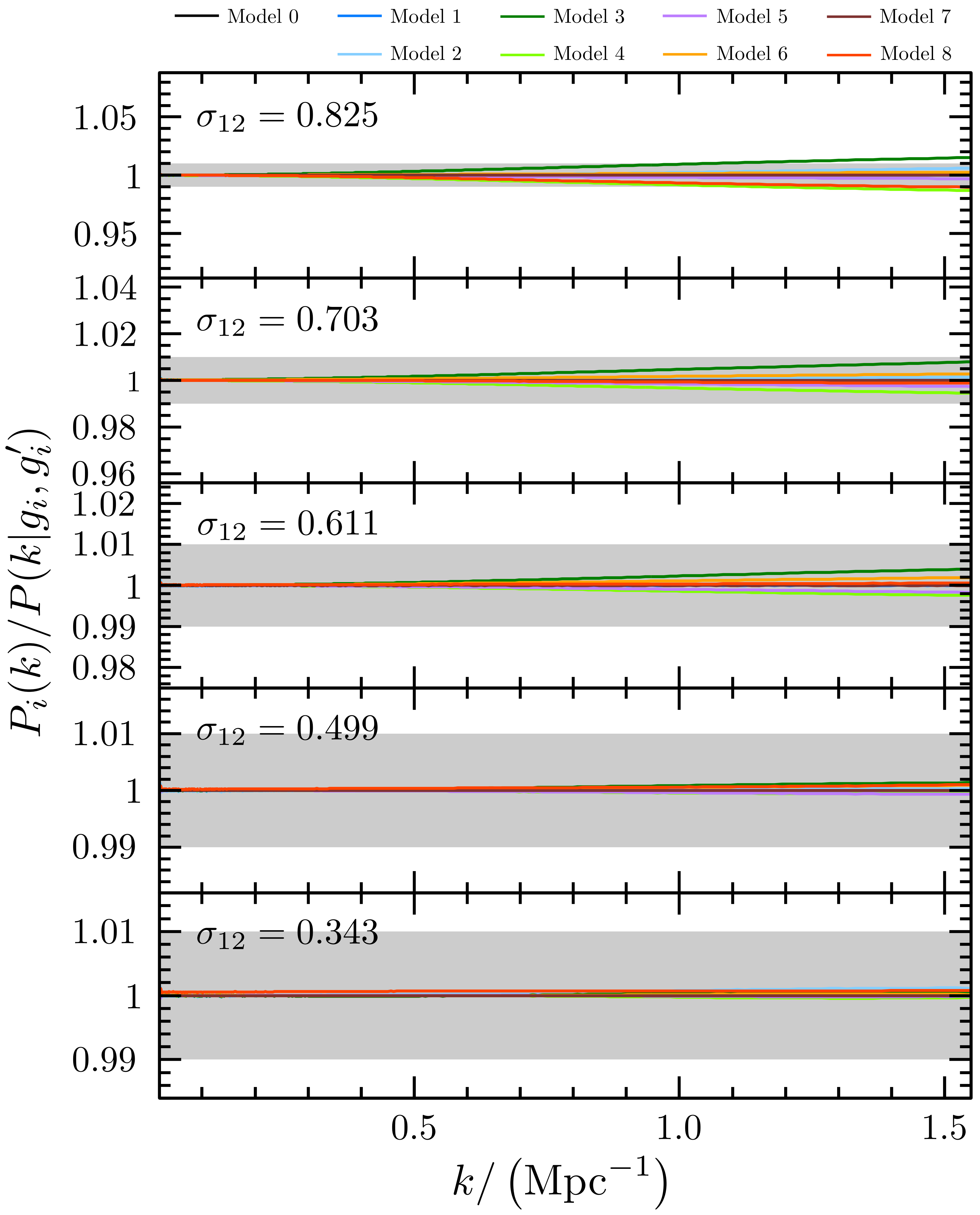

The peculiar velocity field

- Modelling peculiar velocities is essential to analyse redshift-space quantities.
- At the linear level, $\boldsymbol{v}$ and δ are linked through the continuity equation.

$$\theta := -\frac{\boldsymbol{\nabla}\cdot\boldsymbol{v}}{af(a)H(a)} \longrightarrow P_{\theta\theta}(k) = P_{\theta\delta}(k) = P_{\delta\delta}(k)$$

- Considering $\ln\sigma_{12}$ as a time variable

$$\boldsymbol{\Upsilon} = \frac{\mathrm{d}\boldsymbol{x}}{\mathrm{d}\ln\sigma_{12}} = \frac{\mathrm{d}\boldsymbol{x}}{\mathrm{d}t}\frac{\mathrm{d}t}{\mathrm{d}\ln\sigma_{12}} = \frac{\boldsymbol{v}}{af(a)H(a)}$$

- The rescaled velocities $\boldsymbol{\Upsilon}$ follow the evolution mapping relation.

$$\theta = -\boldsymbol{\nabla}\cdot\boldsymbol{\Upsilon}$$

The peculiar velocity field

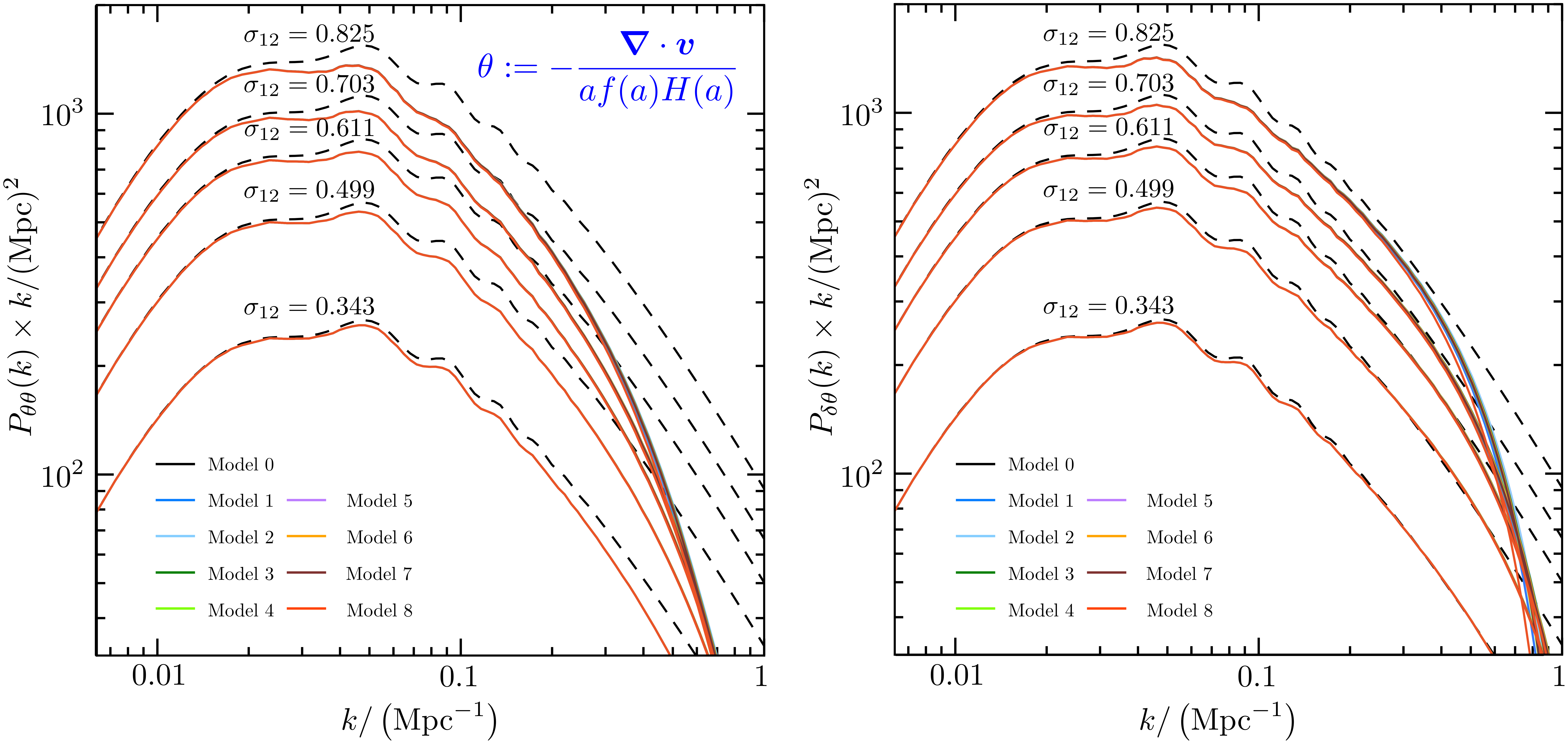

Esposito et al. (2024)

The peculiar velocity field

- Deviations from a perfect degeneracy follow a similar pattern as $P_{\delta\delta}(k)$.
- With the appearance of vorticity, the trend in the deviations is reverted.
- For each model, the maximum deviations are smaller than for $P_{\delta\delta}(k)$.
- The differences can also be described in terms of $\Delta g(\sigma_{12})$ and $\Delta g'(\sigma_{12})$

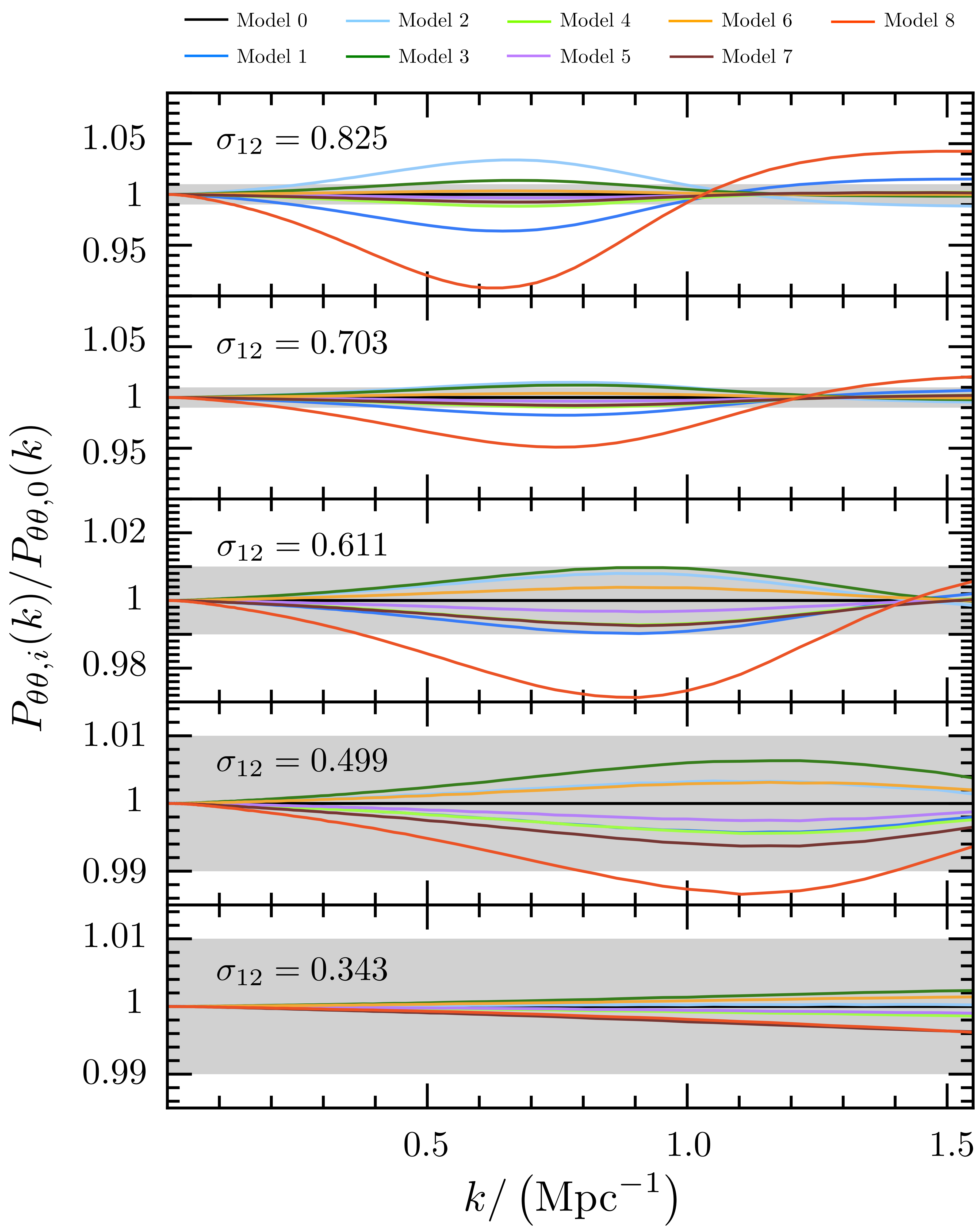

Esposito et al. (2024)

The peculiar velocity field

- Deviations from a perfect degeneracy follow a similar pattern as $P_{\delta\delta}(k)$.
- With the appearance of vorticity, the trend in the deviations is reverted.
- For each model, the maximum deviations are smaller than for $P_{\delta\delta}(k)$.
- The differences can also be described in terms of $\Delta g(\sigma_{12})$ and $\Delta g'(\sigma_{12})$.

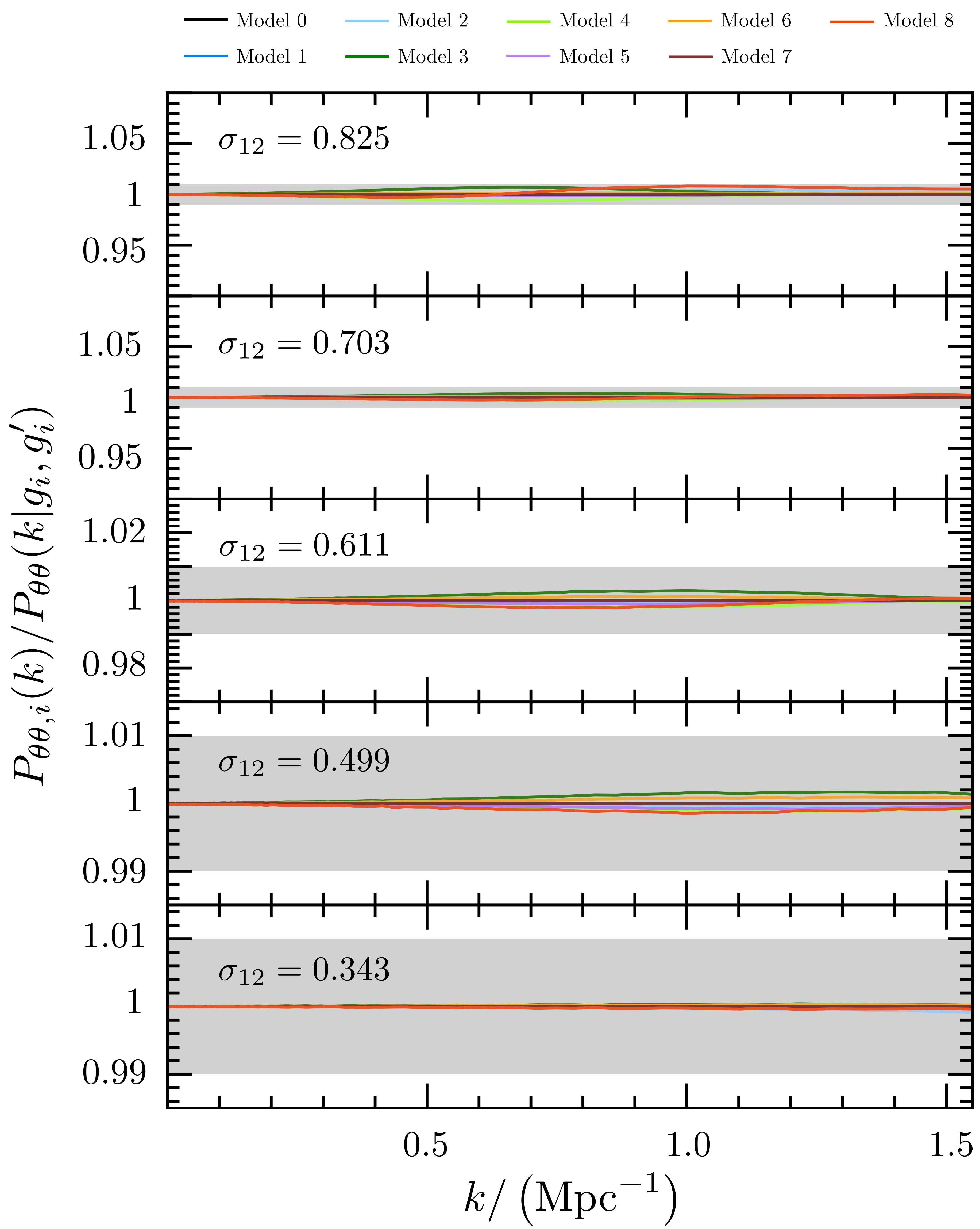

Esposito et al. (2024)

Beyond two-point statistics

- Evolution mapping describes the full density field.
- It can be used to describe multiple statistics.

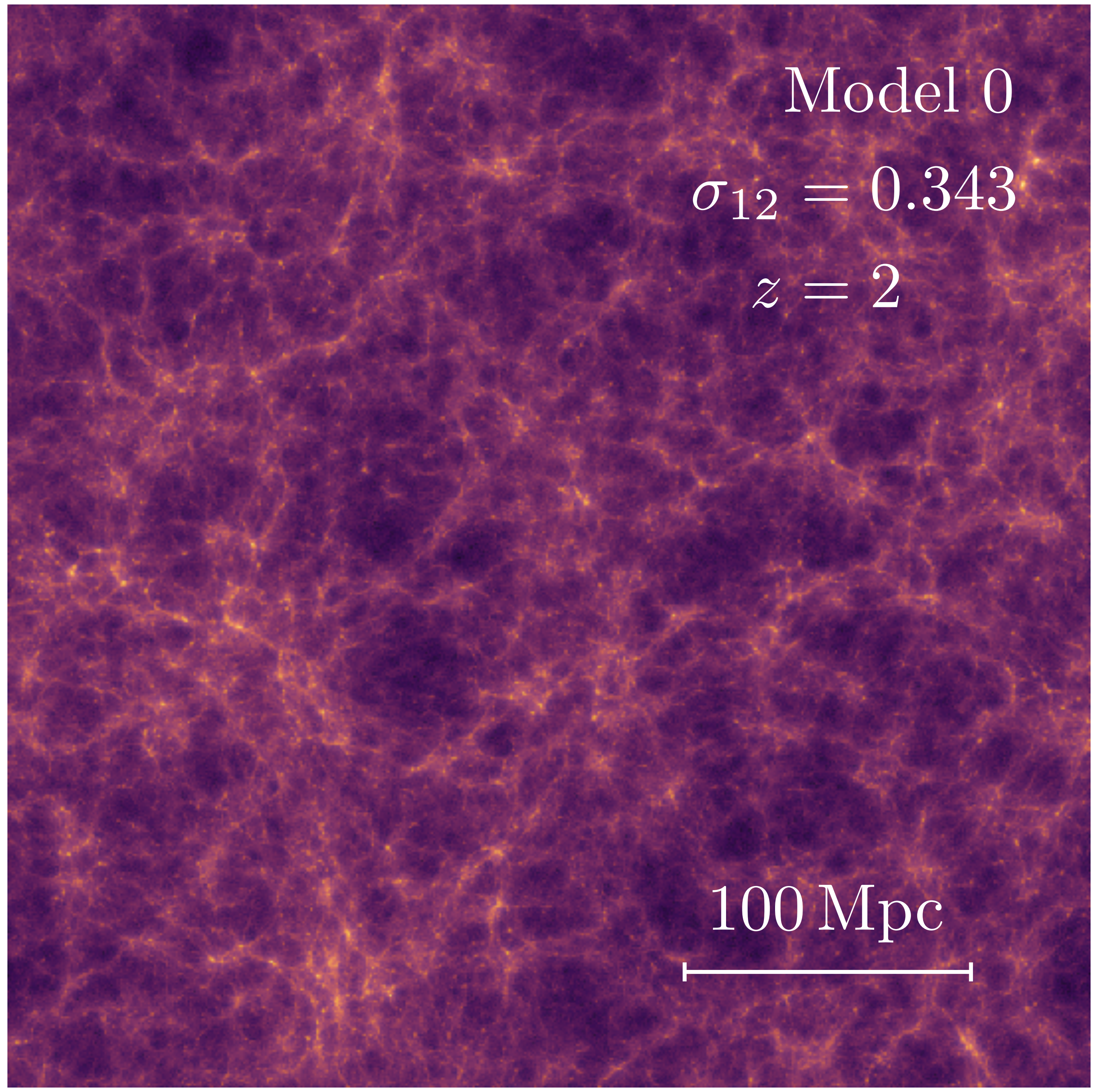

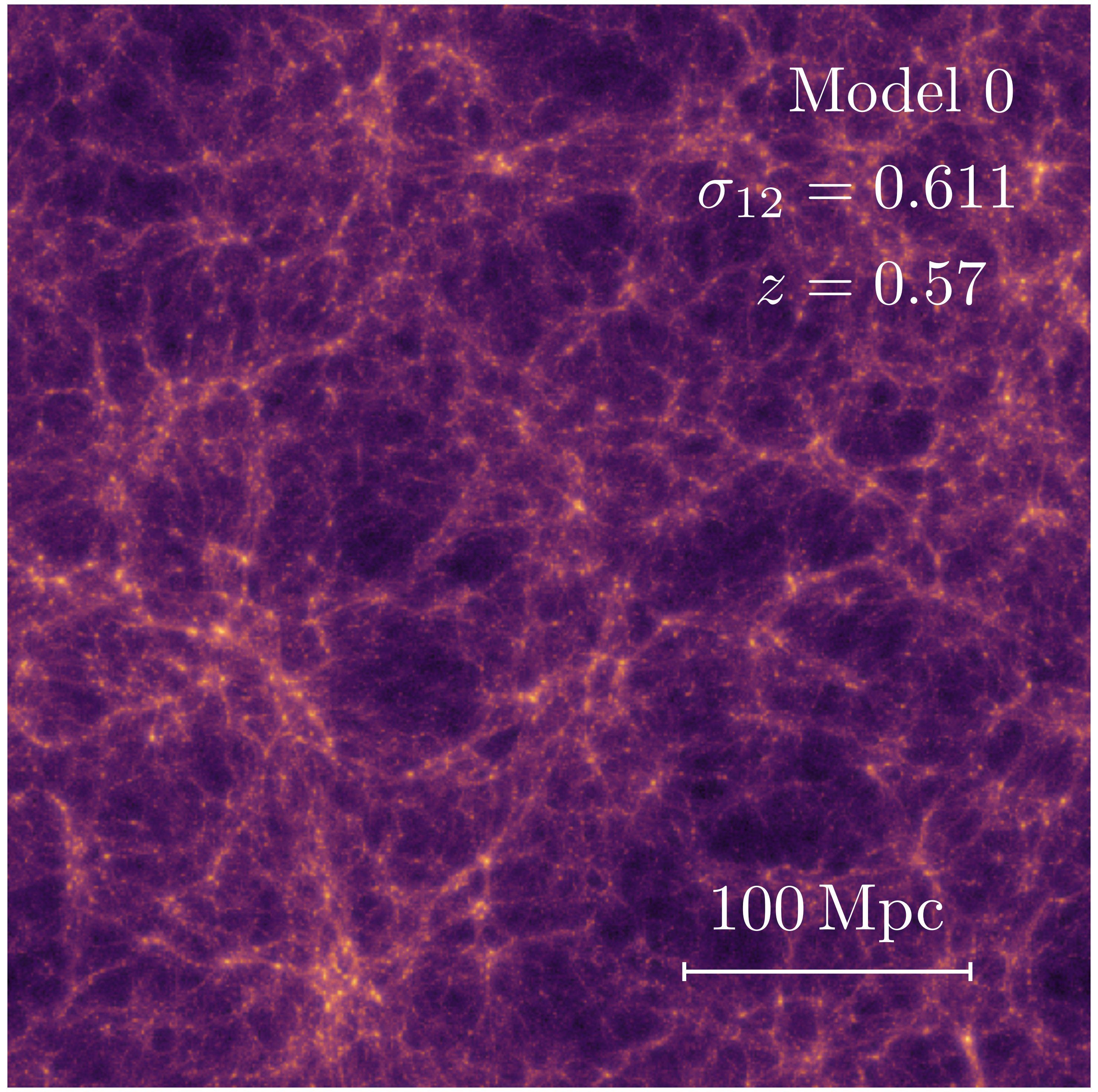

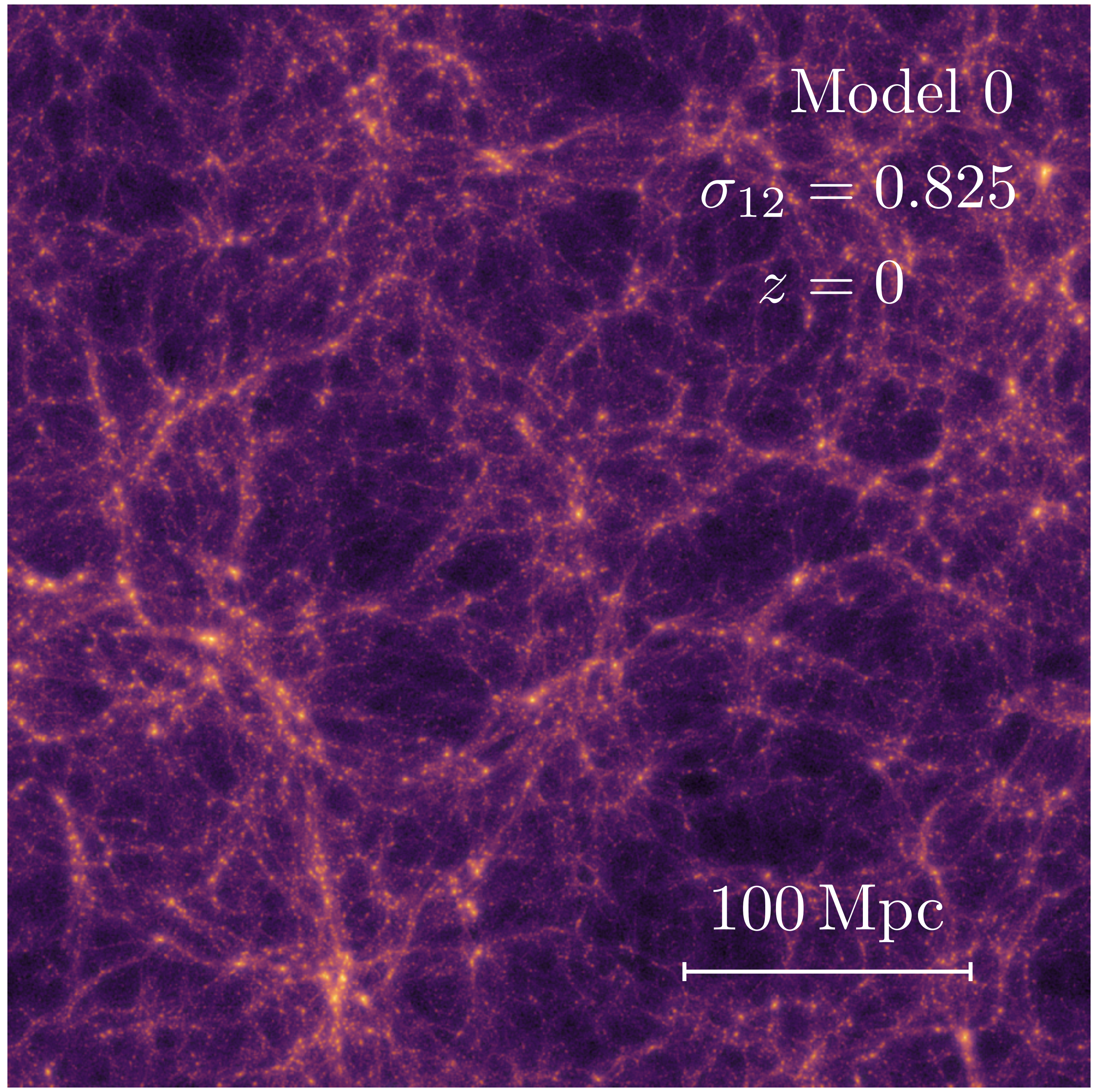

Beyond two-point statistics

- Evolution mapping describes the full density field.
- It can be used to describe multiple statistics.

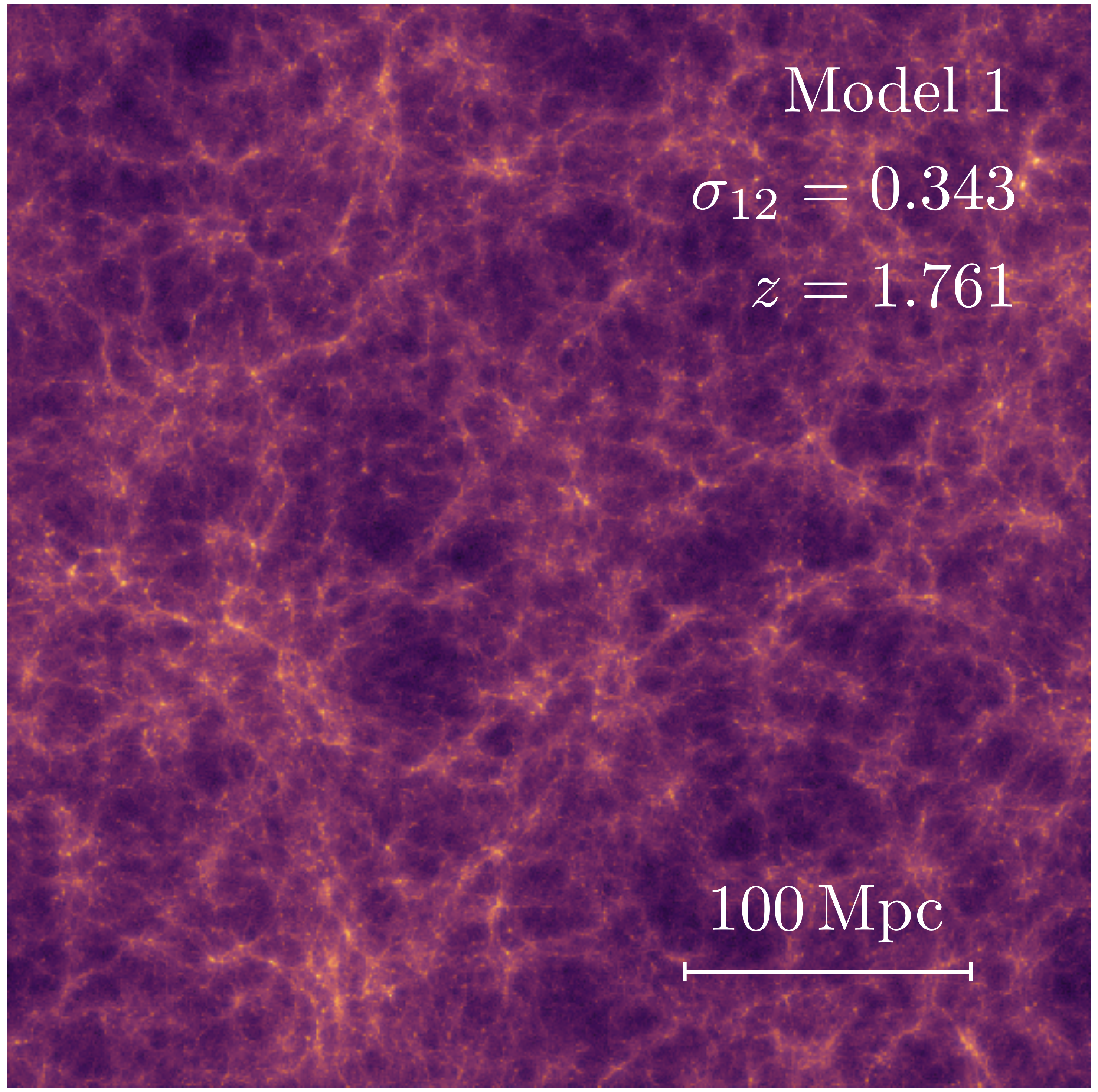

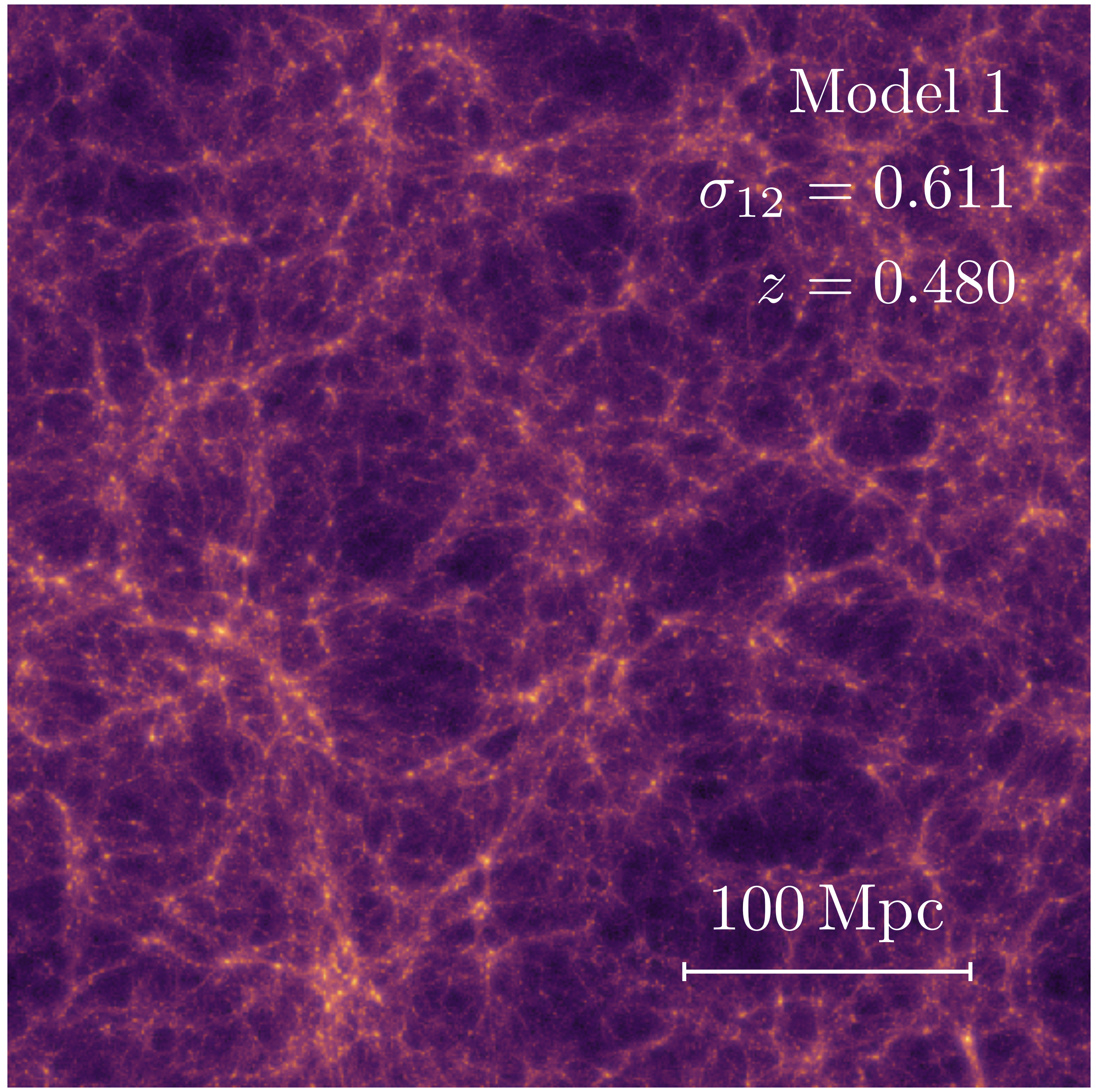

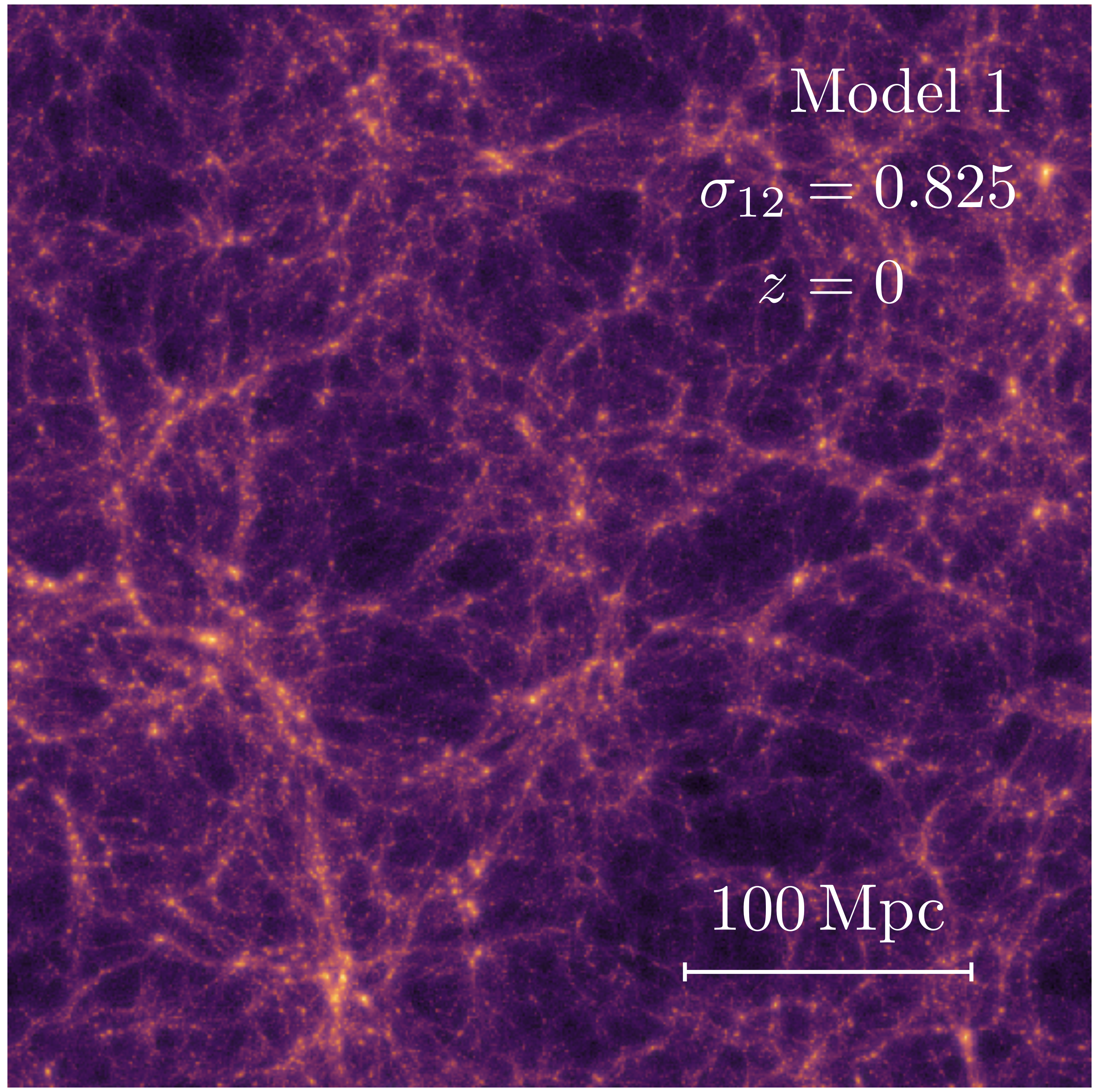

Emulating the non-linear $P(k)$

Standard approach: $\boldsymbol{\Theta} = (\underbrace{\omega_c, \omega_b, n_s}_{\text{shape}}, \underbrace{\omega_K, \omega_{DE}, w_0, w_a, \ldots}_{\text{evolution}}, z)$

Evolution mapping: $\boldsymbol{\Theta} = (\omega_c, \omega_b, n_s, \sigma_{12})$

ALETHEIA

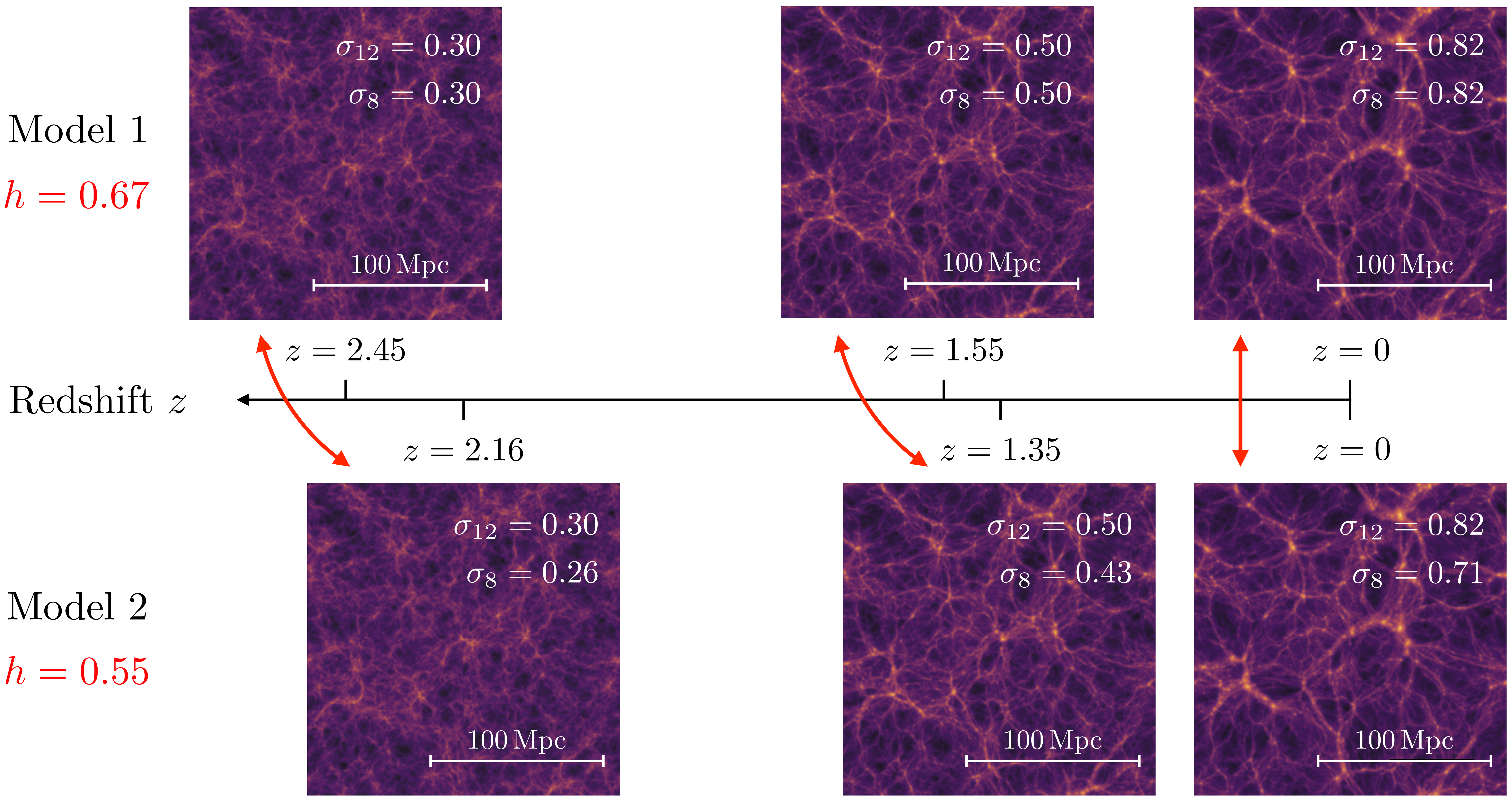

Evolution mapping reduces the required number of parameters to describe $P(k|z)$.

Emulator results must be corrected by $\Delta g(\sigma_{12})$

COMET: Emulating perturbation theory

- Evaluation of $P_\ell(k|z)$ takes a few seconds -> MCMC analyses require a few days.
- For PT models, evolution mapping is exact.
- For a reference set $\mathbf{\Theta}_{\mathrm{e},0}$, we sample

$$\mathbf{\Phi} = (\mathbf{\Theta}_{\mathrm{s}}, \sigma_{12}, f)$$

- COMET is available as a Python package `https://pypi.org/project/comet-emu/`
- New versions adding ω_ν (Pezzotta+ in prep.) and config. space (Semenaite+ in prep.)

COMET - Cosmological Observables Modelled by Emulated perturbation Theory

Parameter	Min. emulator range	Max. emulator range
ω_b	0.0205	0.02415
ω_c	0.085	0.155
n_s	0.92	1.01
σ_{12}	0.2	1.0
f	0.5	1.05

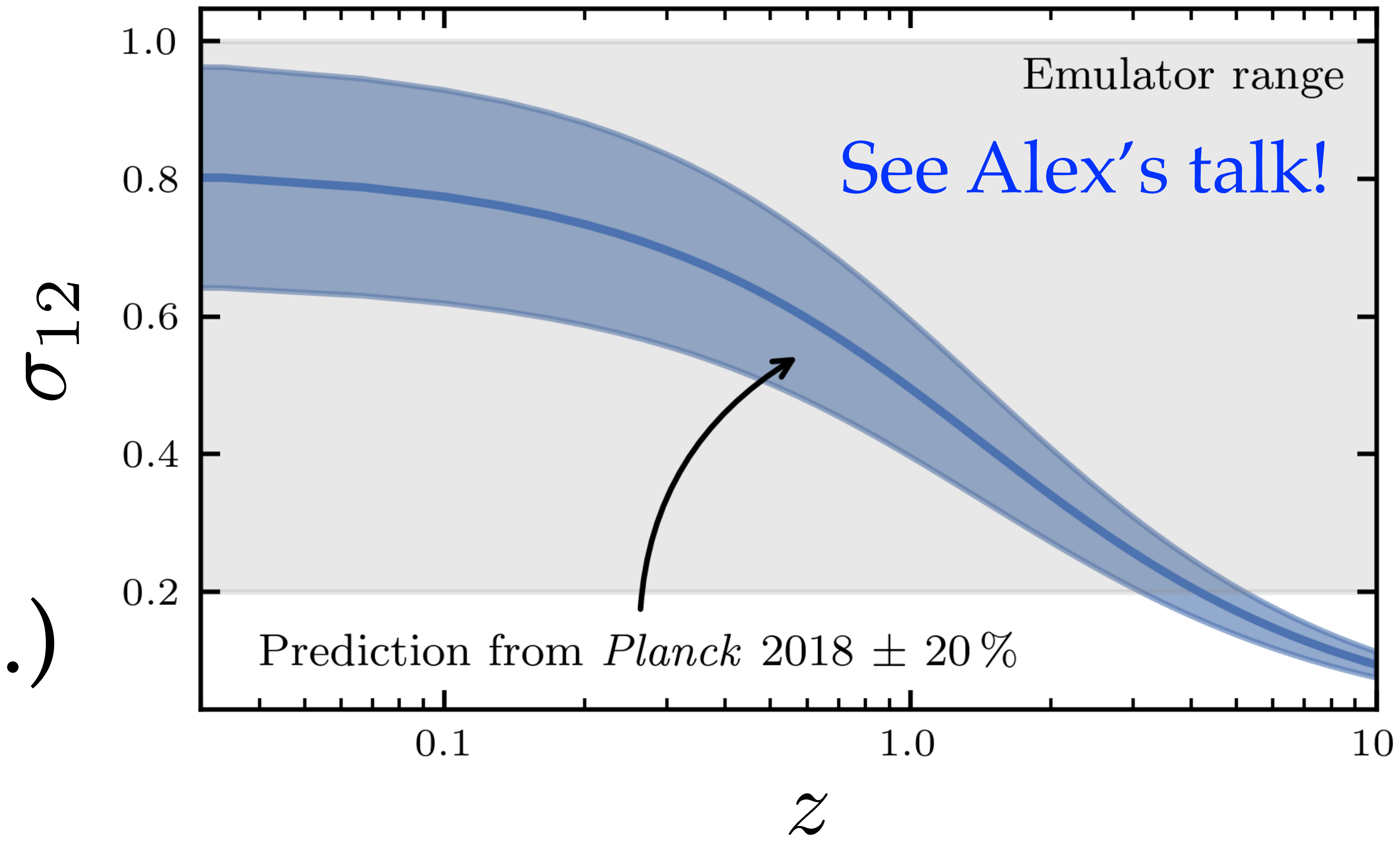

Eggemeier et al. (2022)

Field-level emulation

The computational cost of N-body simulations hinders the use of SBI.

CNNs can reproduce full N-body simulations based on their linear inputs (e.g., He et al. 2018, Jamieson et al. 2023).

Evolution mapping can help to generalise these results.

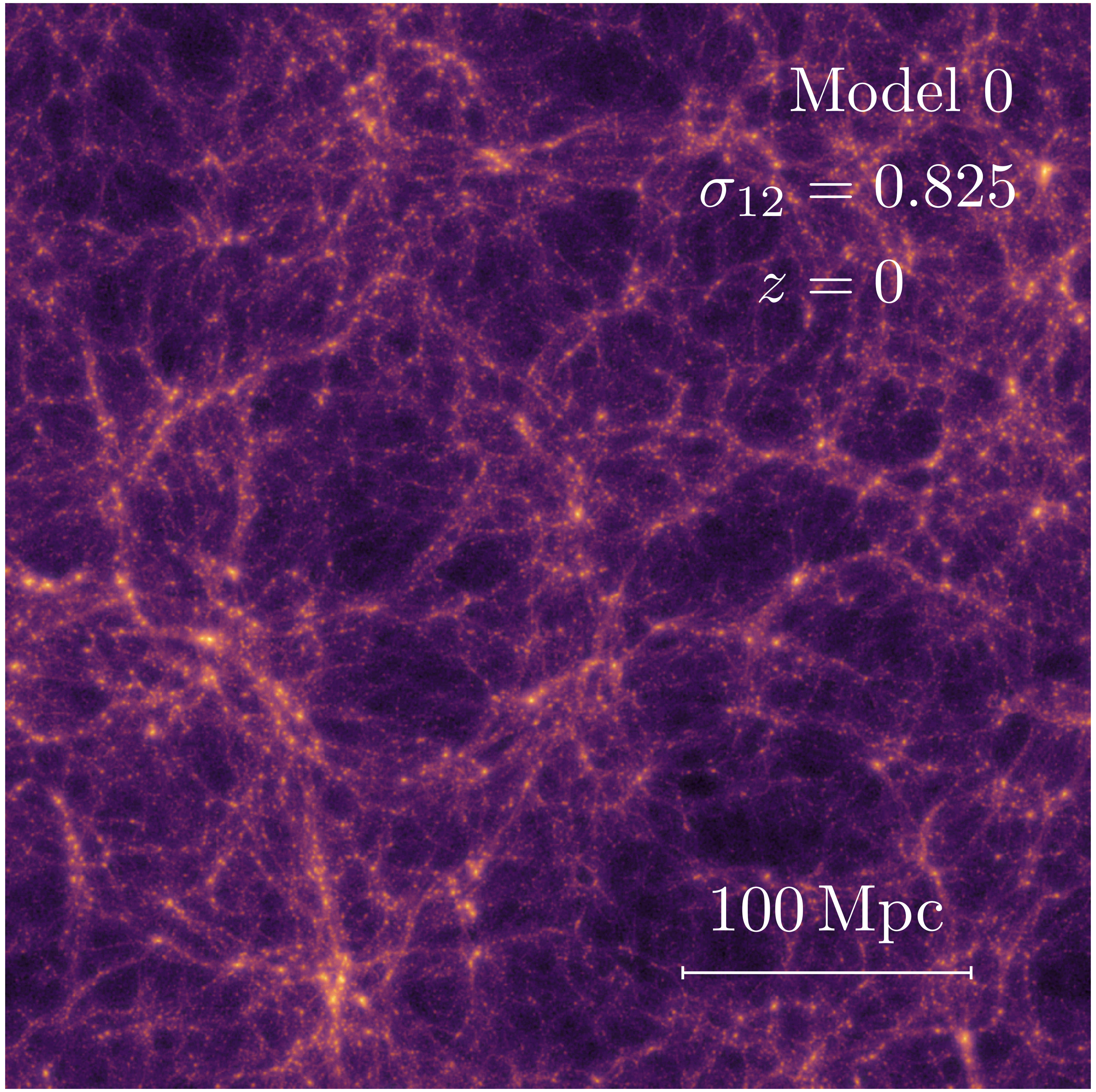

Field-level emulation

Input: 2LPT particle positions

$\boldsymbol{x}_{\rm in} = \boldsymbol{x}_{\rm 2LPT}$

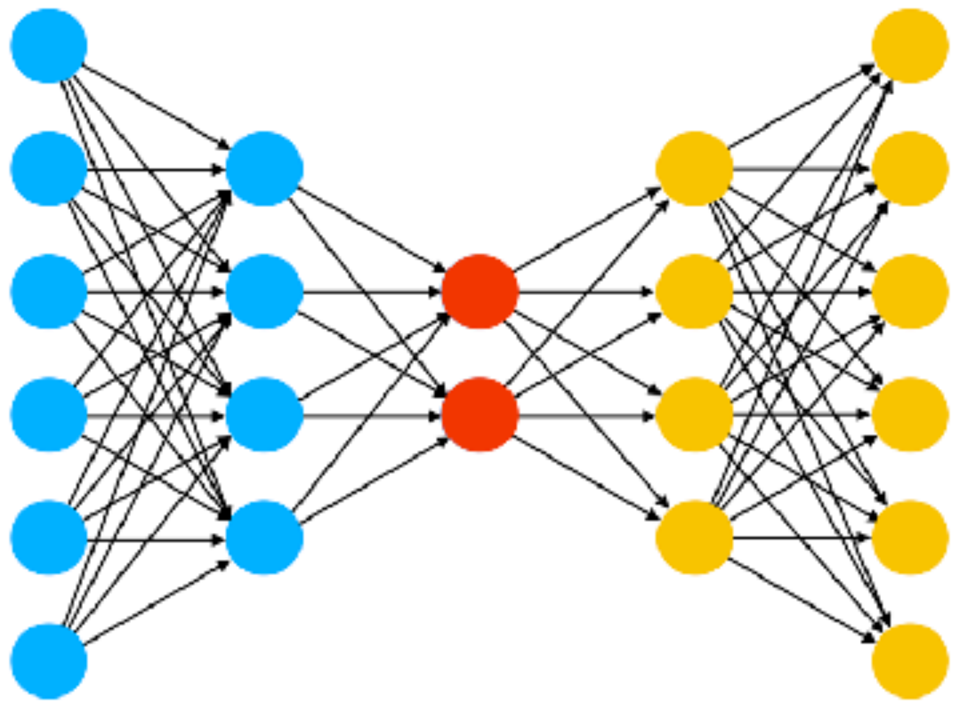

Output: shift to N-body particle position

$\boldsymbol{x}_{\rm out} = \boldsymbol{x}_{\rm Nbody} - \boldsymbol{x}_{\rm 2LPT}$

Preliminary!

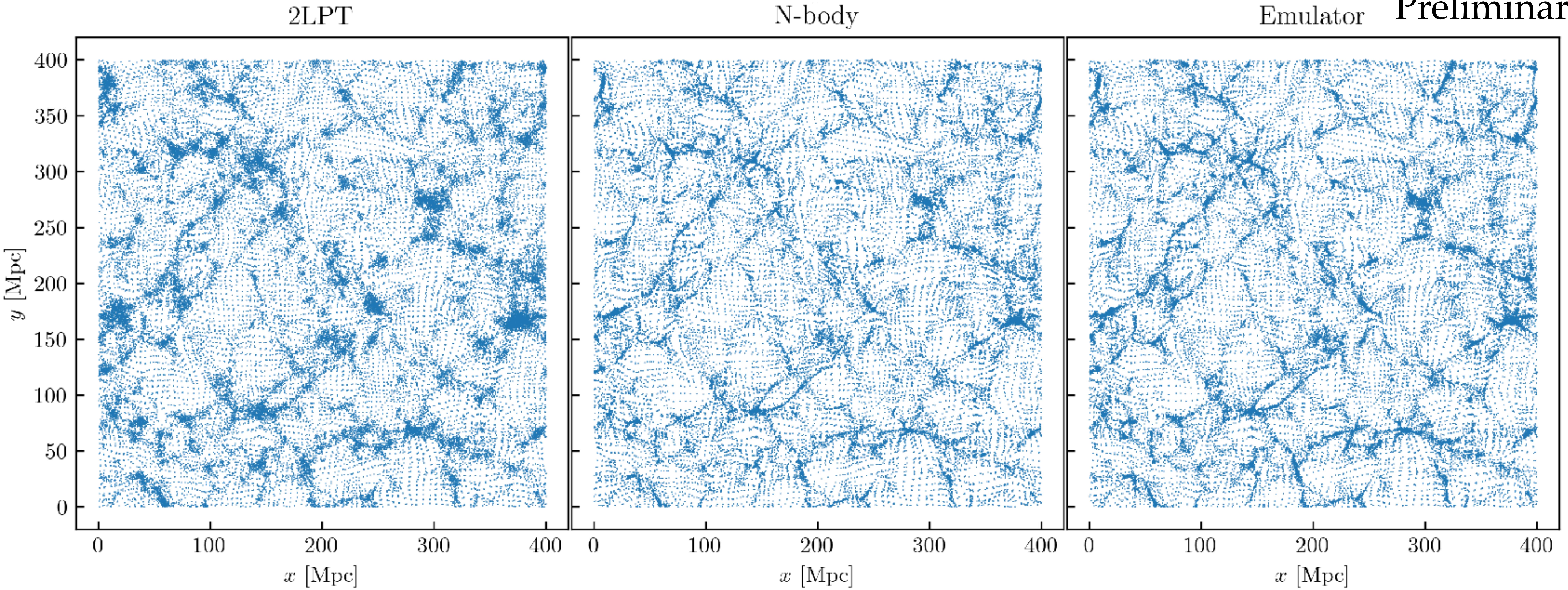

Correa et al. (in prep.), Perez Fernandez et al. (in prep.)

Field-level emulation

- Preliminary results show good performance.
- Currently studying the cosmological dependency of the results

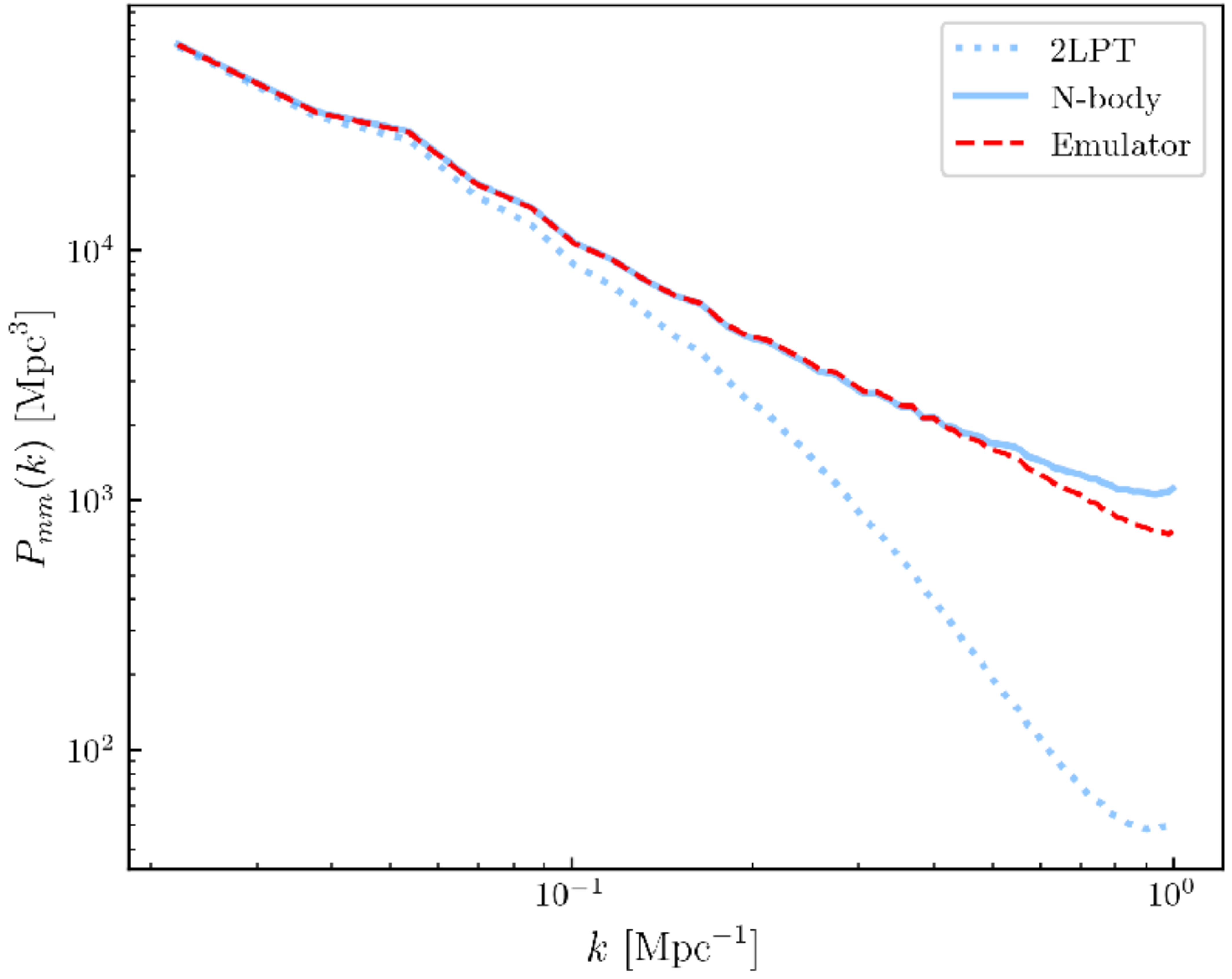

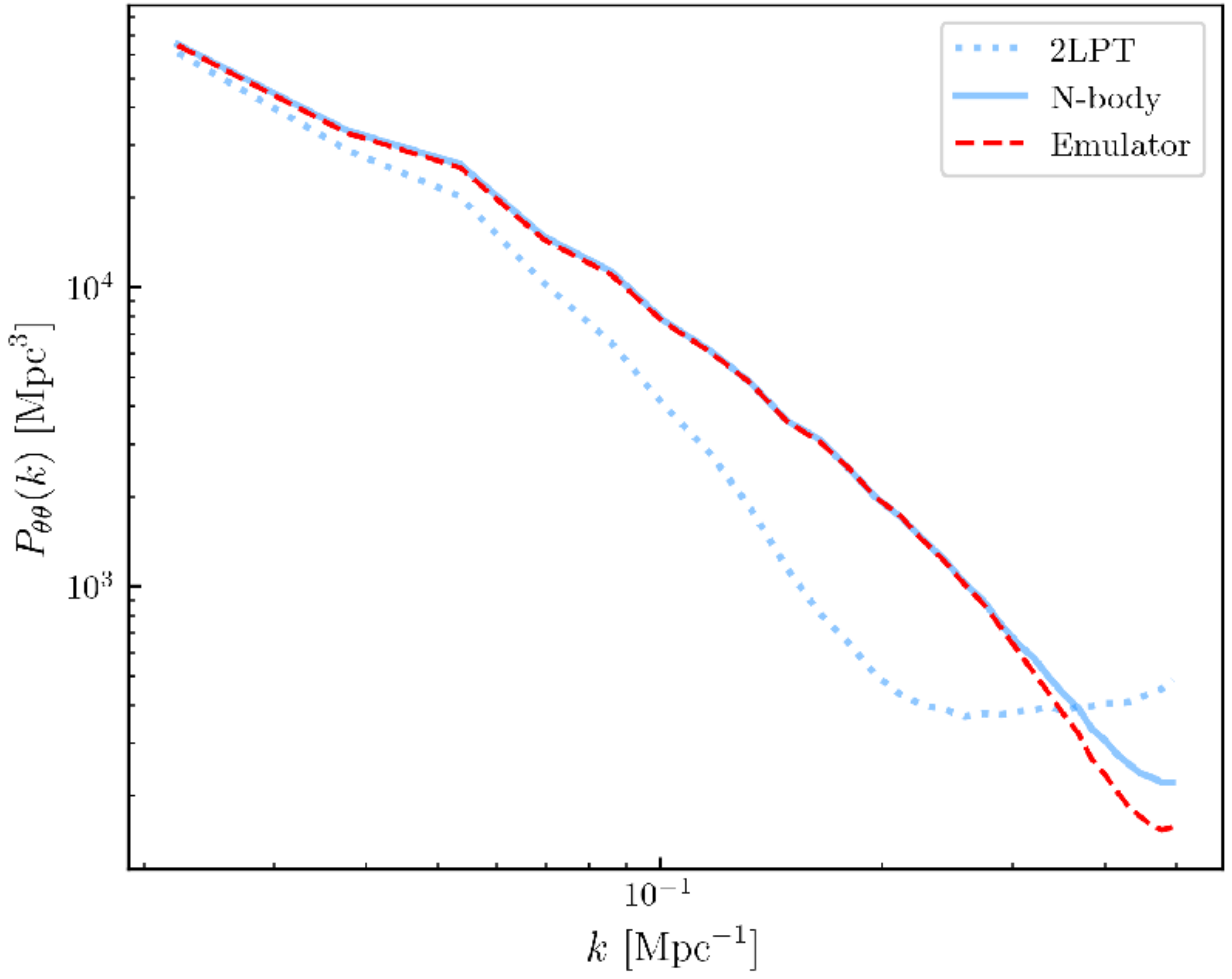

Correa et al. (in prep.),
Perez Fernandez et al. (in prep.)

Field-level emulation

- Preliminary results show good performance.
- Currently studying the cosmological dependency of the results
- Main parameter controling the emulator's performance is $\sigma_{12}(z)$.
- Testing the impact of different structure formation histories.
- Apply to extensions of ΛCDM.

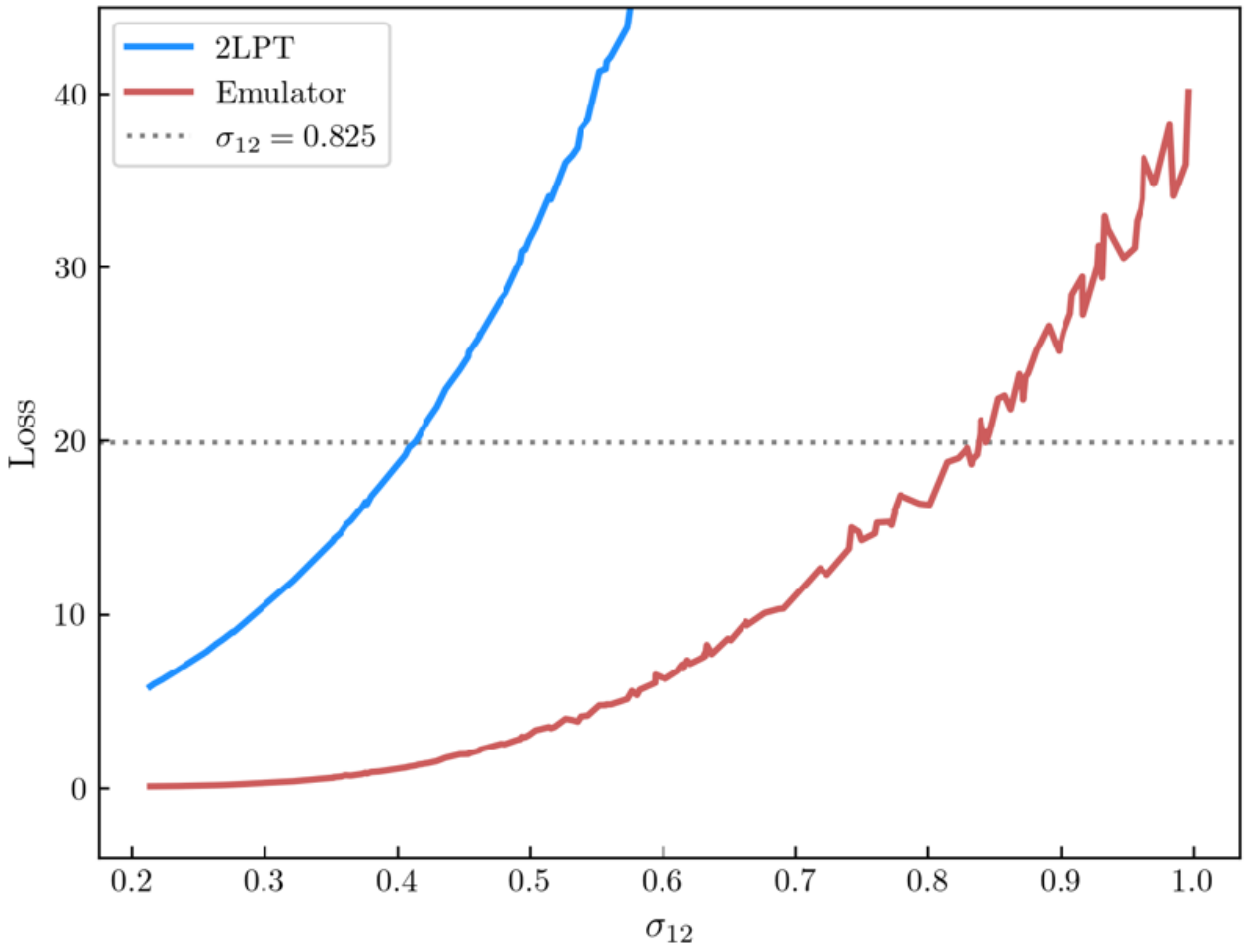

Correa et al. (in prep.),
Perez Fernandez et al. (in prep.)

The information content of $P(k, \mu)$

- Parameter degeneracies are modified for biased tracers in redshift-space

$$P_{\rm gg}(k,\mu) = \left(b_1\sigma_{12} + f\sigma_{12}\mu^2\right)^2 \frac{P_{\rm mm}(k)}{\sigma_{12}^2}$$

- For fixed $\boldsymbol{\Theta}_{\rm s}$, models with the same values of $b_1\sigma_{12}$ and $f\sigma_{12}$ are identical.

- The BAO signal provides constraints on

$$D_{\rm M}(z)/r_{\rm d} \qquad\qquad D_H(z)/r_{\rm d}$$

- The broad-band shape of $P_{\rm gg}(k,\mu)$ contains weak information on the shape parameters (e.g., $n_{\rm s}$).

LSS analysis methods

“Full-modelling” approach:

- Select parameter space to be explored: e.g., ΛCDM, $\boldsymbol{\Theta} = (\omega_{\rm b}, \omega_{\rm c}, \omega_{\rm DE}, n_{\rm s}, A_{\rm s})$
- Theoretical predictions directly compared against clustering data.

“Template” approach:

- Assume a fixed template cosmology.
- Differences between data and the template are compressed into:

$$D_{\rm M}(z)/r_{\rm d},\ D_H(z)/r_{\rm d},\ f\sigma_{8/h}(z)$$

- *Shapefit* includes two parameters, m, n, describing the shape of $P(k)$

Full-modelling LSS analyses

- Most LSS studies used full modelling (Sánchez+ 2017, Semenaite+ 2022, 2023)
- Focus on accuracy of the constraints: analyses used LSS + CMB data.
- Current focus: asses the consistency between different data sets.
- Several BOSS-only analyses (d'Amico+ 2020, Ivanov+ 2020, Tröster + 2020, …)

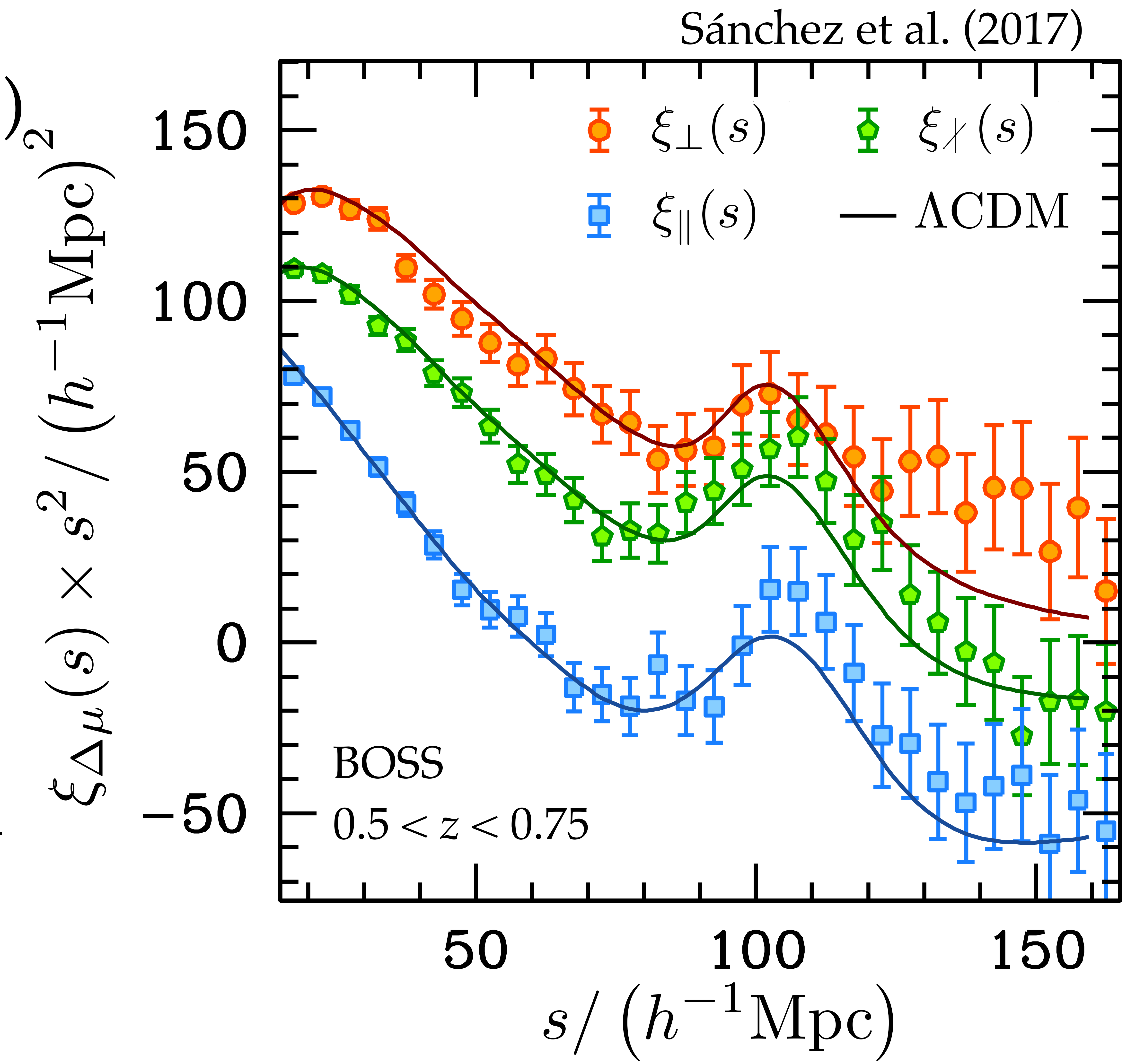

Template LSS analyses

- In the standard template analysis, h is kept fixed.
- The constraints on $f\sigma_{8/h}(z)$ depend on that assumption.
- The correct error on $f\sigma_{8/h}(z)$ should be marginalised over h.
- The effect disappears when expressed in terms of $f\sigma_{12}(z)$.

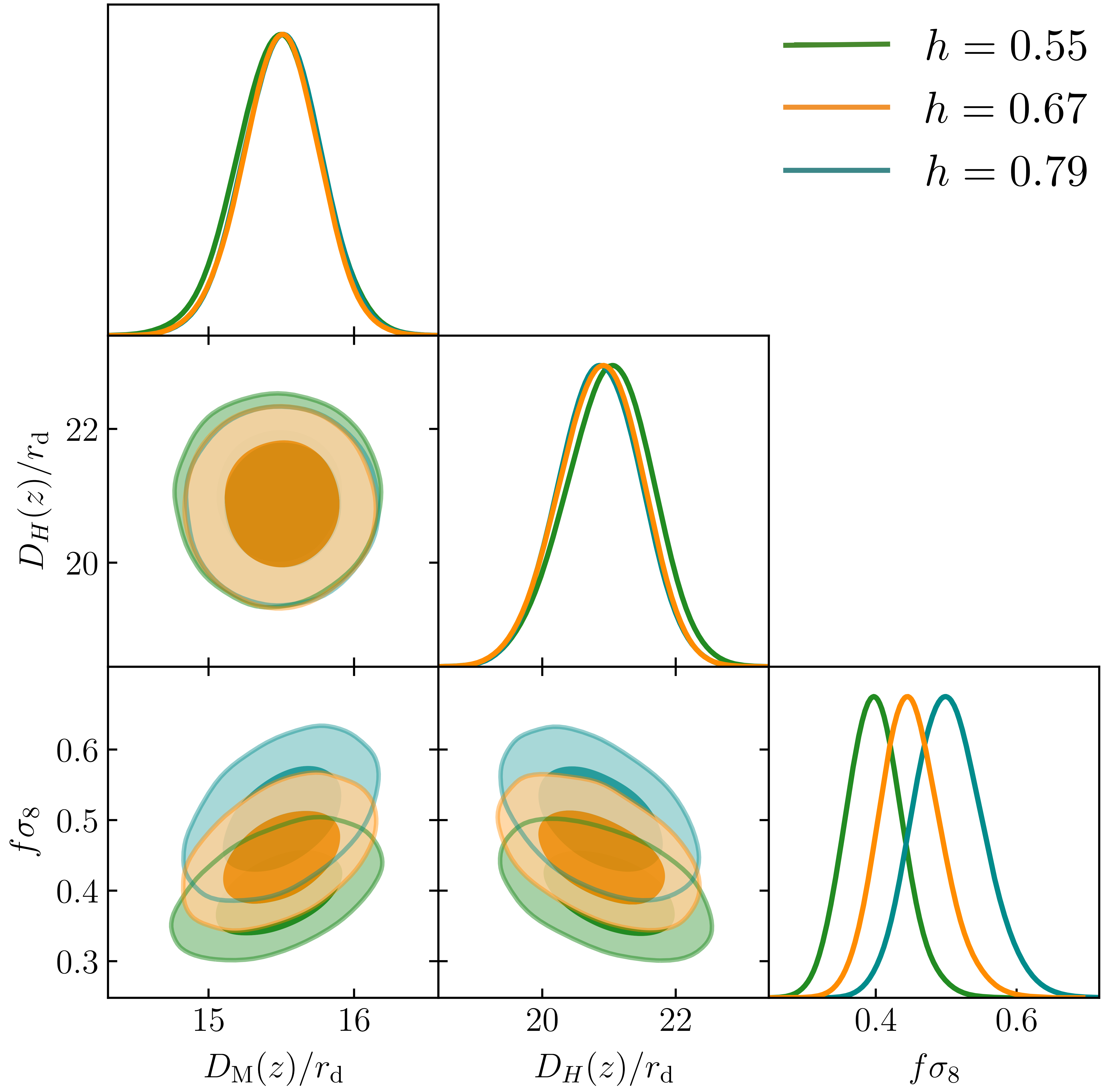

Template LSS analyses

- In the standard template analysis, h is kept fixed.
- The constraints on $f\sigma_{8/h}(z)$ depend on that assumption.
- The correct error on $f\sigma_{8/h}(z)$ should be marginalised over h.
- The effect disappears when expressed in terms of $f\sigma_{12}(z)$.

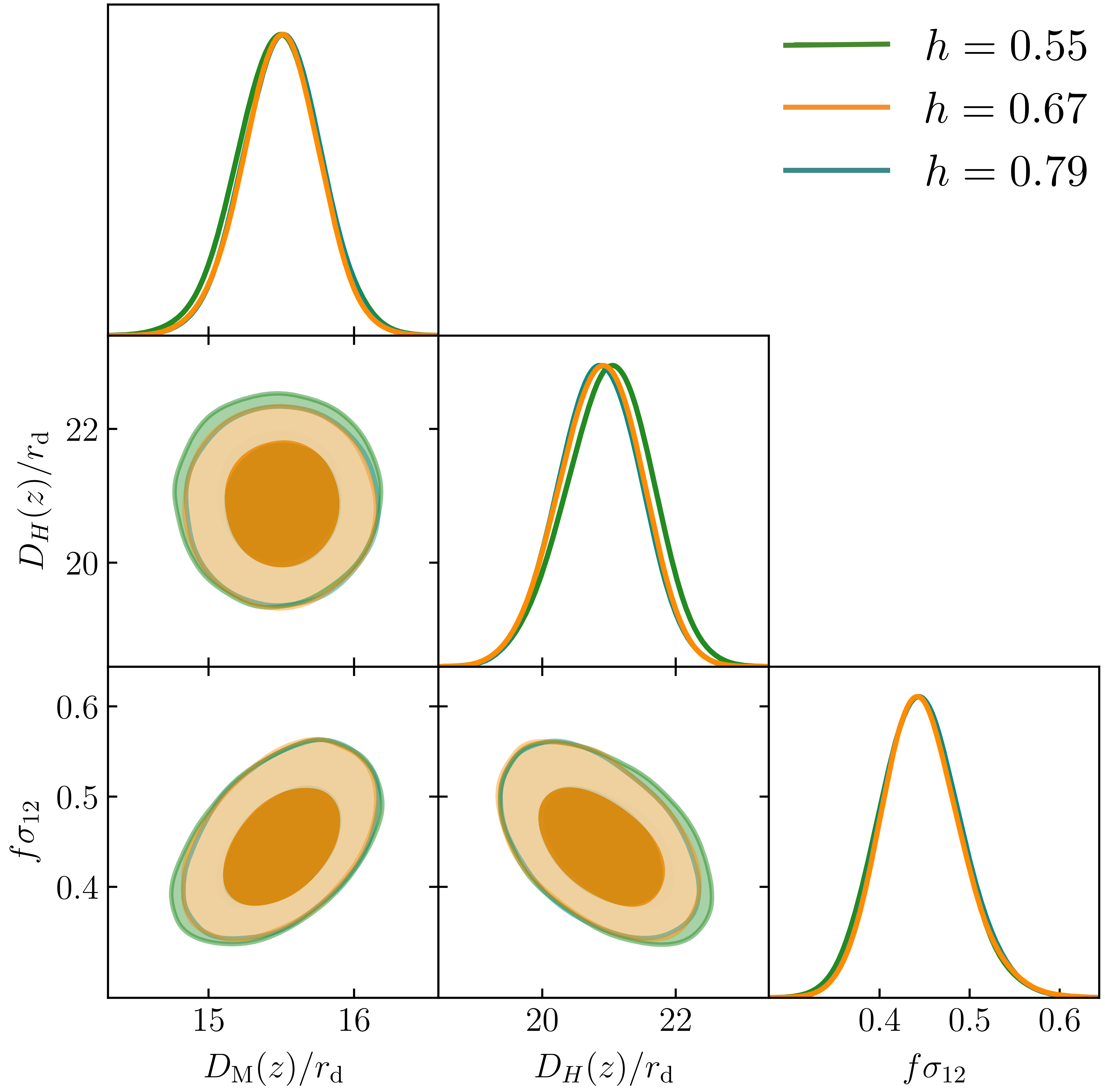

Template LSS analyses

- Constraints on *w*CDM:

$$\boldsymbol{\Theta} = (\omega_{\rm b}, \omega_{\rm c}, \omega_{\rm DE}, n_{\rm s}, A_{\rm s}, w_{\rm DE})$$

- Planck + BOSS (high-z)
  - *Full-modelling* analysis:

$$w_{\rm DE} = -1.04 \pm 0.082$$

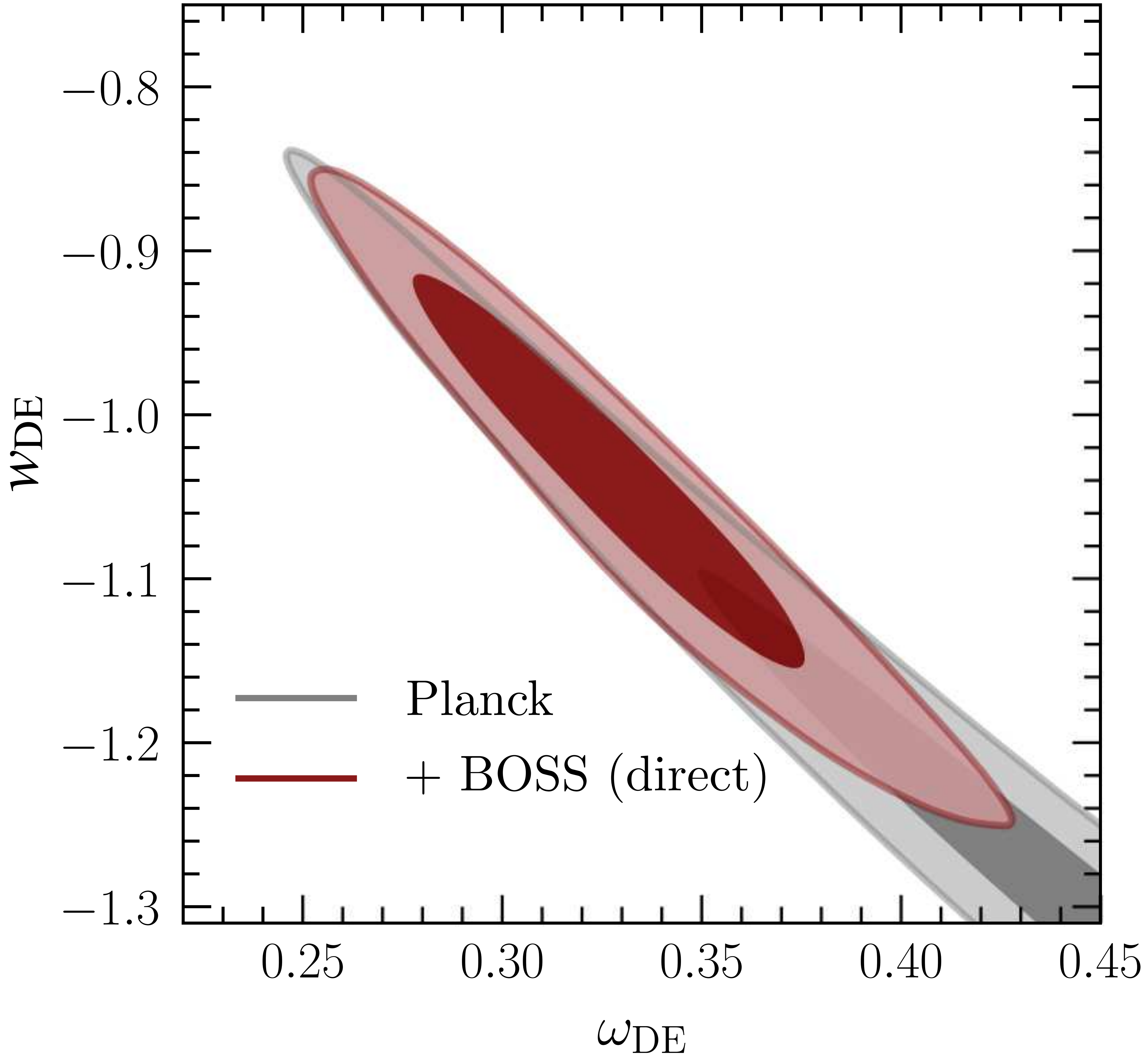

Template LSS analyses

- Constraints on wCDM:

$$\mathbf{\Theta} = (\omega_\mathrm{b}, \omega_\mathrm{c}, \omega_\mathrm{DE}, n_\mathrm{s}, A_\mathrm{s}, w_\mathrm{DE})$$

- Planck + BOSS (high-z)
  - *Full-modelling* analysis:

$$w_\mathrm{DE} = -1.04 \pm 0.082$$

  - *Template* analysis using $f\sigma_{8/h}(z)$:

$$w_\mathrm{DE} = -1.02 \pm 0.065$$

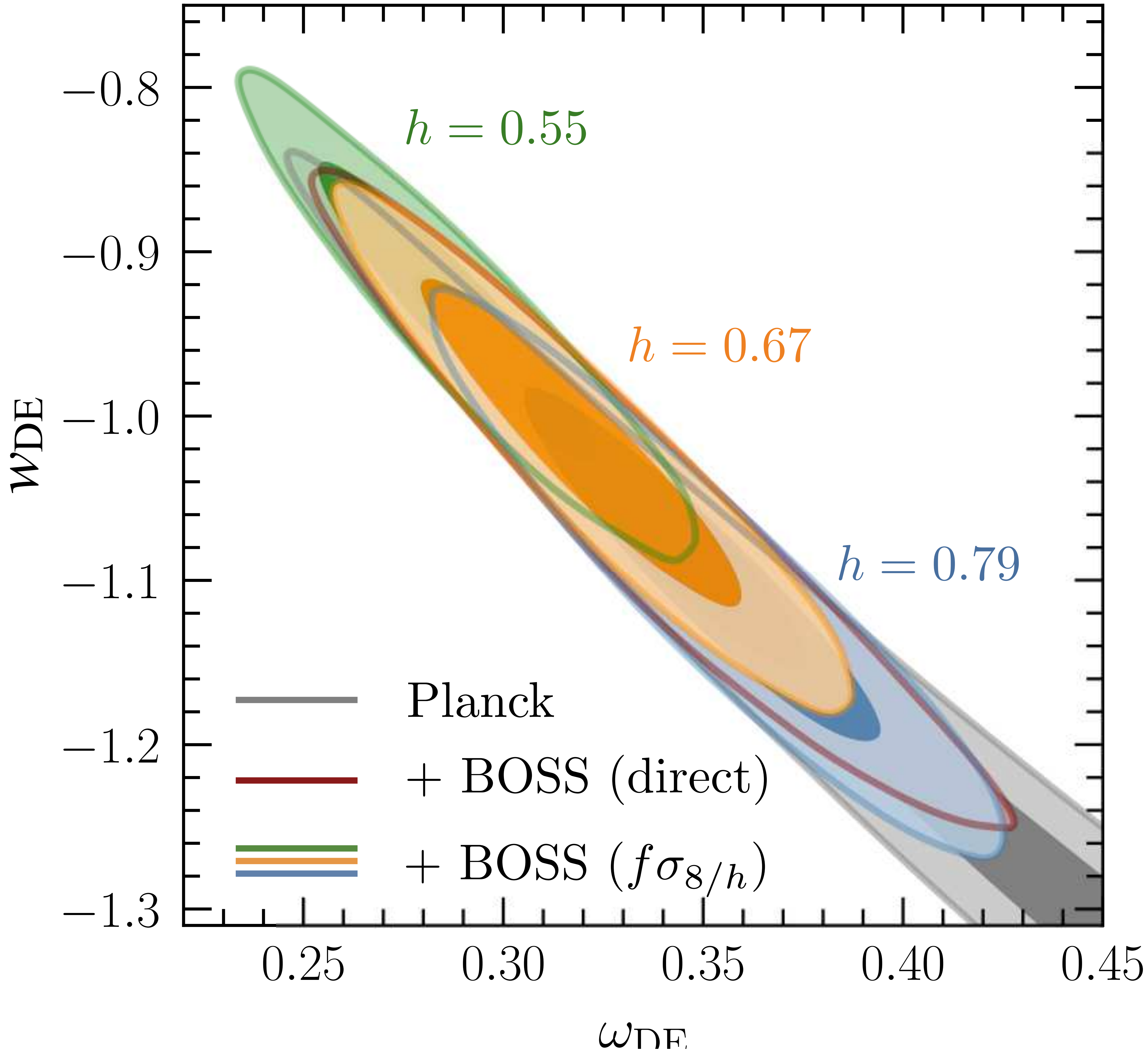

Template LSS analyses

- Constraints on *w*CDM:

$$\mathbf{\Theta} = (\omega_b, \omega_c, \omega_{DE}, n_s, A_s, w_{DE})$$

- Planck + BOSS (high-z)
  - *Full-modelling* analysis:

$$w_{DE} = -1.04 \pm 0.082$$

  - *Template* analysis using $f\sigma_{8/h}(z)$:

$$w_{DE} = -1.02 \pm 0.065$$

  - *Template* analysis using $f\sigma_{12}(z)$:

$$w_{DE} = -1.05 \pm 0.083$$

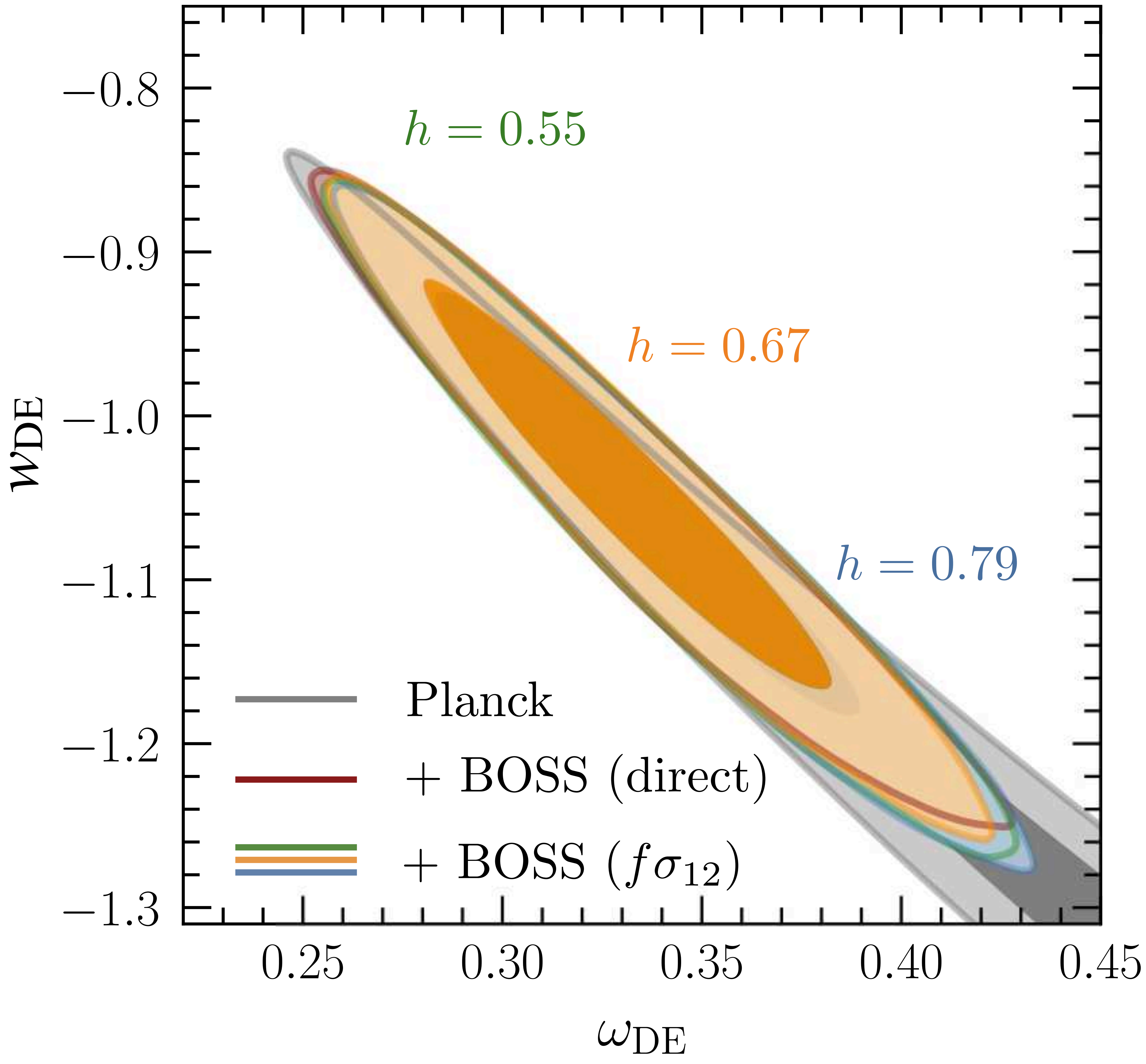

Template LSS analyses

- Gil-Marin+ (2020) proposed to use $f\sigma_{8,q}$

$$\sigma_{8,q}^2 = \int_0^\infty \mathrm{d}k\, k^2 P_\mathrm{L}(k)\, W^2(s_8 q k),$$

where $s_8 = (8/h)\,\mathrm{Mpc}$ and $q^3 = q_\perp^2 q_\parallel$

- This quantity cannot be used as the standard $f\sigma_{8/h}(z)$.

- Interpreting $f\sigma_{8,q}$ as $f\sigma_{8/h}$ leads to

$$w_\mathrm{DE} = -1.03 \pm 0.065$$

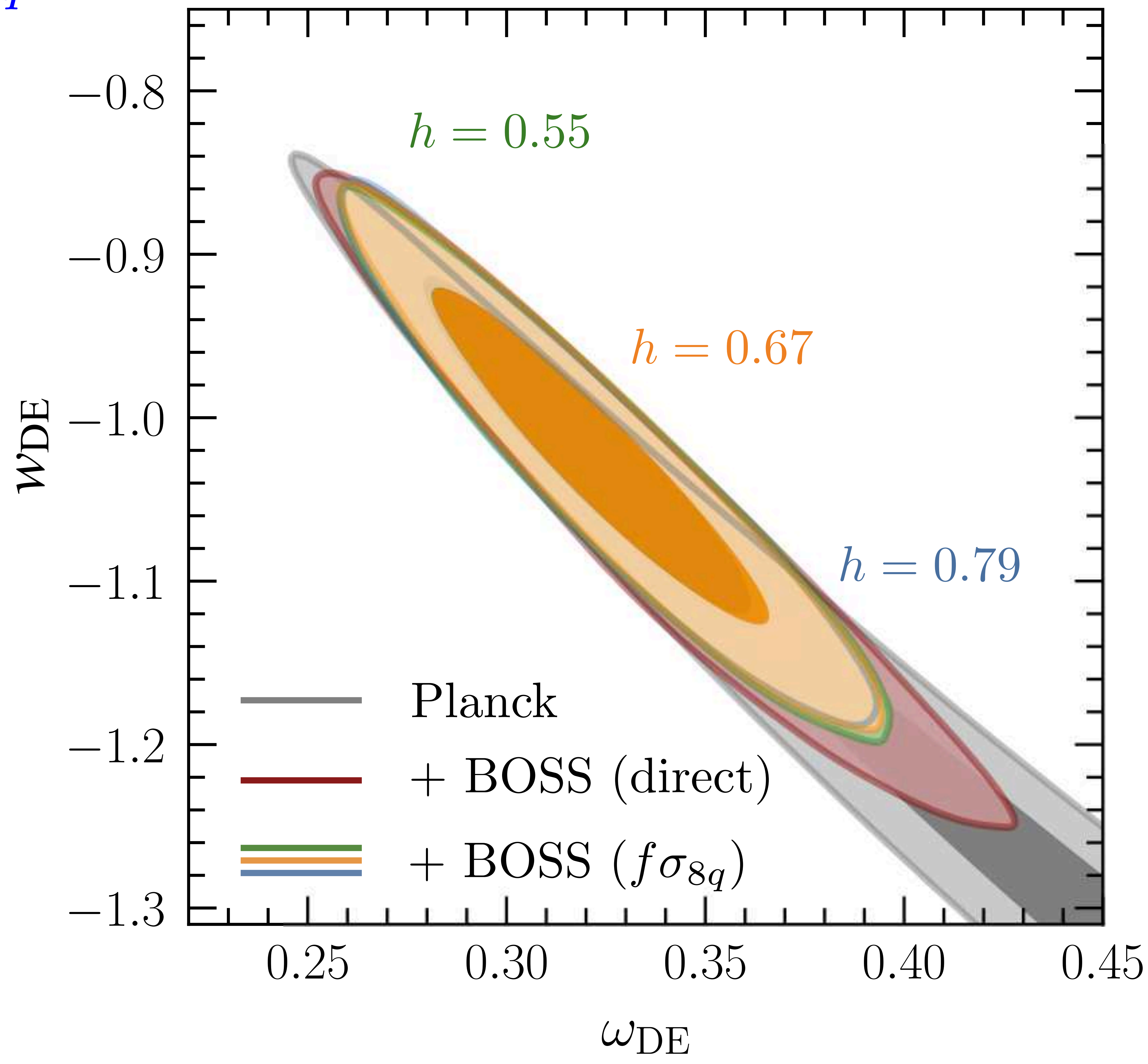

Template LSS analyses

- Brieden+ (2021, SHAPEFIT) proposed to use instead

$$s_{\rm d} = \frac{r_{\rm d}}{r_{\rm d,fid}}\,(8/h)\,{\rm Mpc}$$

- A scale proportional to $r_{\rm d}$ means using a reference scale in Mpc.

- Multiple analyses still quote their results in terms of $f\sigma_{8/h}(z)$.

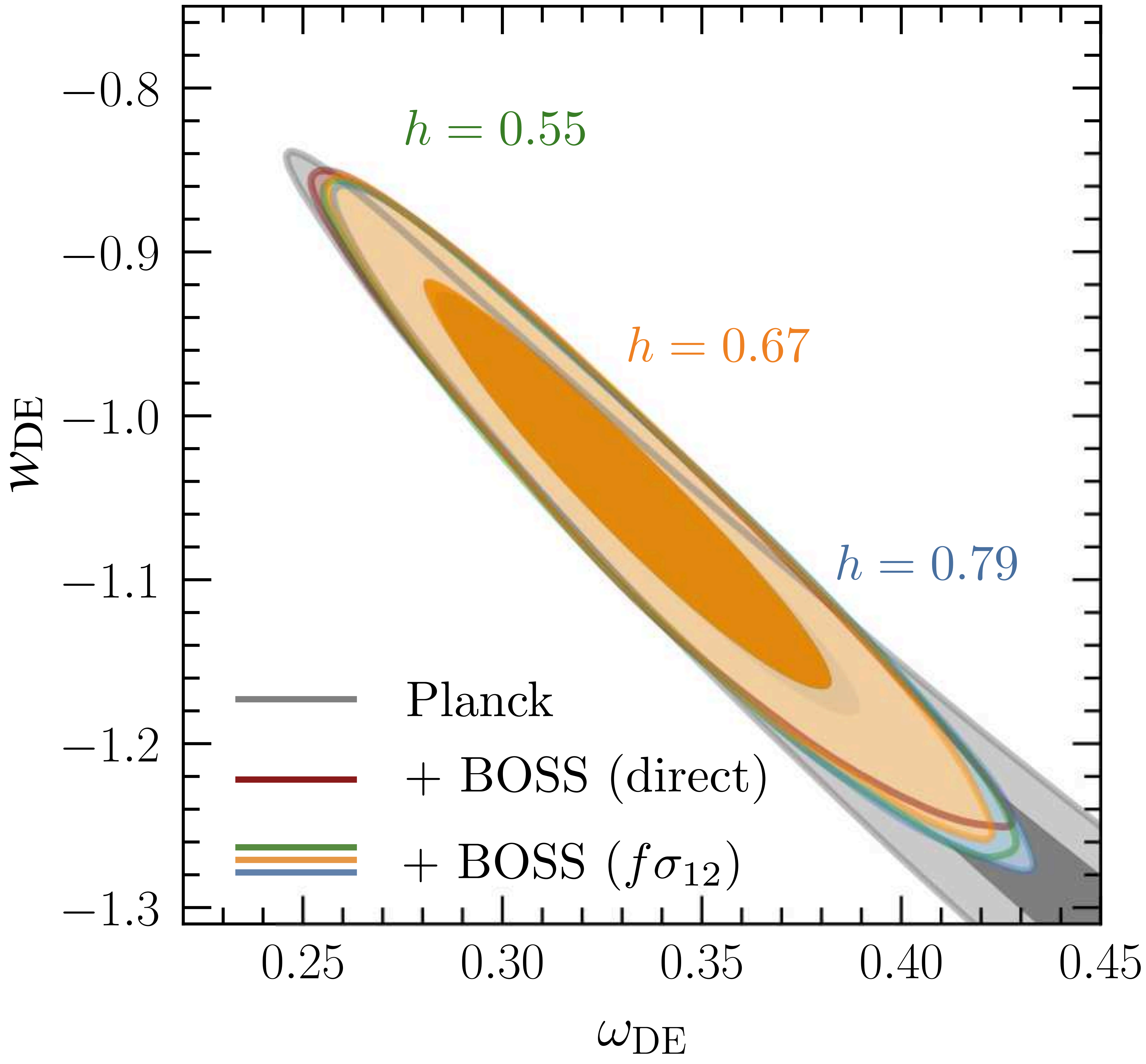

Final remarks

- Evolution mapping: we classify parameters into ***Shape*** and ***evolution*** based on their impact on $P_{\mathrm{L}}(k|z)$.
- At the linear level, $\boldsymbol{\Theta}_{\mathrm{e}}$ follow a perfect degeneracy, described by σ_{12}.
- This is partially inherited by the non-linear density field, with deviations sensitive to the suppression $g(a) = D(a)/a$.
- We are using evolution mapping to build new descriptions of the non-linear matter density field.
- This approach can help us to better understand the information content of all clustering measurements.